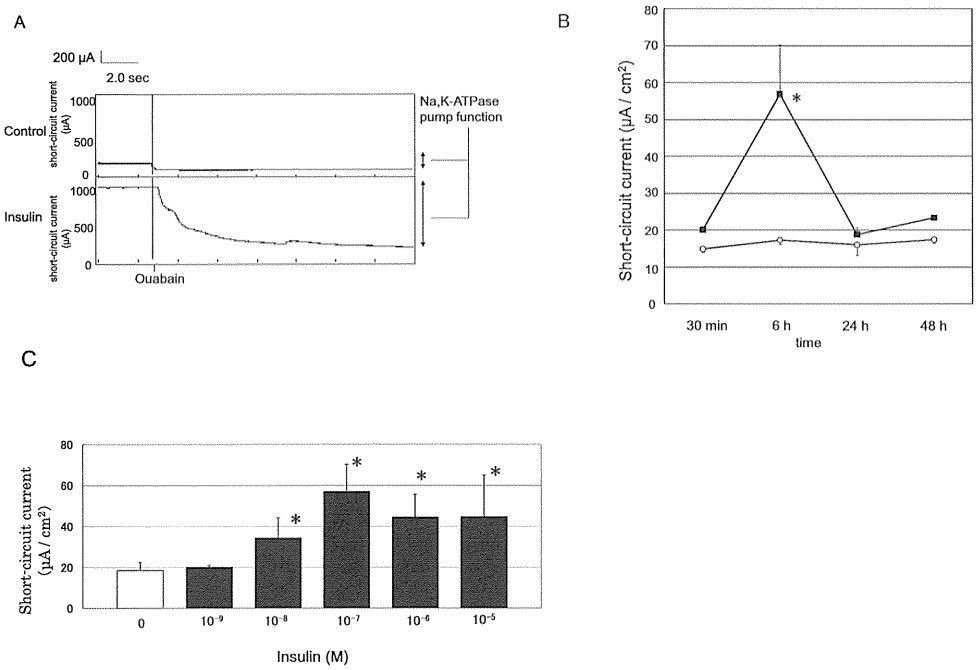

FIGURE 2. Effect of insulin on the pump function of cultured mouse corneal endothelial cells. (**A**) Representative tracings of short-circuit current (μA/well) obtained with cell monolayers in a Ussing chamber. The insert well membrane growth area was 4.67 cm^2. The cells were incubated in the absence (*upper*) or presence (*lower*) of 0.1 μM insulin. Pump function attributable to Na,K-ATPase activity was calculated as the difference in short-circuit currents obtained before and after the addition of ouabain. (**B**) Pump function (μA/cm^2) attributable to Na,K-ATPase activity was determined in the absence (*open circles*) or presence (*closed squares*) of 0.1 μM insulin for the indicated times. Data are mean ± SD of values from of replicates from a representative experiment. $^*P < 0.05$ compared with the corresponding value for cells incubated without insulin (Student's *t*-test). (**C**) Pump function (μA/cm^2) attributable to Na,K-ATPase activity was determined 6 hours after incubation of cells in the presence of the indicated concentrations of insulin. Data are mean ± SD of values of four replicates from four representative experiments. $^*P < 0.05$ for the indicated comparisons (Student's *t*-test).

inhibitor of protein phosphatase 1 (PP1) and protein phosphatase 2A (PP2A), expression of the total Na,K-ATPase α_1-subunit did not change (Fig. 4B), and the insulin-induced dephosphorylation of Na,K-ATPase α_1-subunit was diminished (Fig. 4C).

Effect of Staurosporine, GF109203X, and Okadaic Acid on Insulin-Induced Na,K-ATPase Activation

To test whether the stimulatory effect of insulin on Na,K-ATPase activity was mediated by PKC, we examined the effects of staurosporine and GF109203X. The increase in Na,K-ATPase activity induced by insulin was significantly inhibited by staurosporine and GF109203X (Fig. 5). These results indicated that the increase in Na,K-ATPase activity induced by insulin at a concentration of 0.1 μM was mediated by PKC.

We next examined whether okadaic acid might affect the Na,K-ATPase activation induced by insulin. The activity of Na,K-ATPase at 0.1 μM insulin was significantly reduced in the presence of 1 μM okadaic acid (Fig. 5). These results suggest that the activity of PP1, PP2A, or both is essential to insulin-induced Na,K-ATPase activation.

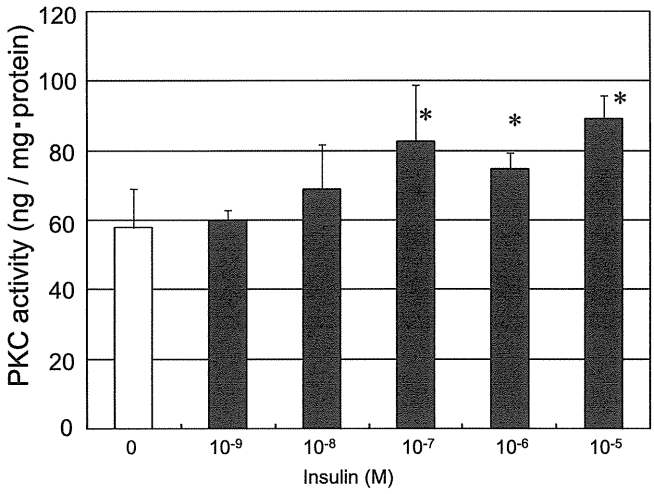

FIGURE 3. Effect of insulin concentration on PKC activity in cultured mouse corneal endothelial cells. Cells were incubated with the indicated concentrations of insulin for 30 minutes, after which the activity of PKC was measured in cell extracts. Data are mean ± SD of values of four replicates from four representative experiments. $^*P < 0.05$ versus the value for cells incubated without insulin (Student's *t*-test).

Effect of Insulin on Na,K-ATPase α_1-Subunit Cell Surface Expression

To determine whether the effect of insulin changes the cell surface expression of the Na,K-ATPase α_1-subunit, we examined the immunocytochemistry of the Na,K-ATPase α1-subunit after insulin treatment in the presence and absence of the inhibitors staurosporine, GF109203X, and okadaic acid. The staining was performed without permeabilization and the majority of observed staining was on the cell surface; thus, inactive Na,K-ATPase was not detected. Insulin-treated corneal endothelial cells expressed the Na,K-ATPase α1-subunit at their lateral cell membranes more than did control cells (Figs. 6A, 6B). In the presence of inhibitors, Na,K-ATPase α1-subunit expression of insulin-treated corneal endothelial cells was weakened at their lateral cell membranes (Figs. 6C–E).

Discussion

In the present study, we show that insulin increases Na,K-ATPase activity and its related pump function in cultured corneal endothelial cells. Changes in Na,K-ATPase activity and pump function under various experimental conditions were well correlated. Our results support the notion that Na,K-ATPase activity is an important determinant of the ability of corneal endothelial cells to maintain the water content of the corneal stroma.[50] Our results suggest that the observed effect of insulin on Na,K-ATPase activity in corneal endothelial cells is transient. A chronic lack of insulin in type 1 diabetes mellitus or a chronic reduced level of insulin signaling by insulin resis-

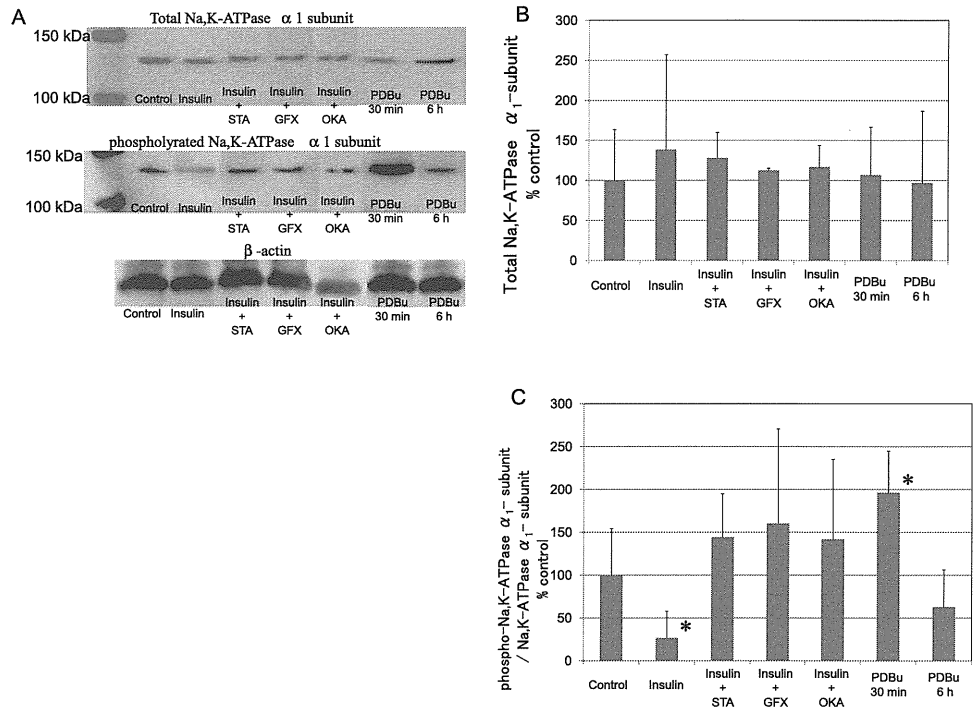

FIGURE 4. Western blot analysis of Na,K-ATPase α_1-subunit and phospho-Na,K-ATPase α_1-subunit expression. (**A**) Representative signals of expression. *Top*: Na,K-ATPase α_1-subunit. *Middle*: phospho-Na,K-ATPase α_1-subunit. *Bottom*: β-Actin. For the following, the relative intensity of each band to β-actin was measured by a densitometer as the expression of Na,K-ATPase α_1 or phospho-Na,K-ATPase α_1-subunit. (**B**) Cells were incubated in the absence (control) or presence of 0.1 μM insulin for 6 hours, 0.1 μM insulin for 6 hours with 30 minutes preincubation of 1 μM staurosporine (insulin+STA), 0.1 μM GF109203X (insulin+GFX), or 1 μM okadaic acid (insulin+OKA), 0.1 μM PDBu for 30 minutes as a positive control, and 0.1 μM PDBu for 6 hours and were then assayed for the expression of Na,K-ATPase α_1-subunit. Data are mean ± SD from five experiments, expressed as a percentage of control. (**C**) The rate of inactive state of Na,K-ATPase α_1-subunit with insulin, insulin+STA, insulin+GFX, insulin+OKA, and PDBu for 30 minutes and 6 hours. Values represent the ratio of phospho-Na,K-ATPase α_1-subunit expression to Na,K-ATPase α_1-subunit expression. Data are mean ± SD of values from five experiments. $^*P < 0.05$ versus the value for cells incubated without insulin (Student's *t*-test).

tance in type 2 diabetes mellitus is essential in the pathogenesis of corneal abnormalities in diabetes.

Insulin has been shown to stimulate the electrogenic sodium transport in a variety of cells.[27–37] In most cases, the increase in Na^+ transport is thought to be a result of the stimulation of the Na,K-ATPase. Various mechanisms of insulin action have been advocated, including changes of the kinetic properties of the enzyme,[28,29] an increase in the intracellular Na concentration, which in turn leads to a subsequent pump stimulation,[30–34] and an increase in the pump concentration at the cell surface by serum and glucocorticoid-dependent kinase (SGK).[35–37] Regardless whether insulin stimulates pump activity by a previous increase in cytosolic Na^+, in its affinity for Na^+, or in pump availability at the cell surface, the insulin receptor signaling cascades must be involved.[27] The signaling cascades include those mediated by protein kinases such as PKC. To date, PKC is regarded to trigger the rapid action of insulin on the Na,K-ATPase and to be involved in the stimulation of the Na,K-ATPase by insulin in muscle cells.[27] Our results suggest that the regulation of Na,K-ATPase activity by insulin in corneal endothelial cells is associated with the active state of the Na,K-ATPase α_1-subunit, and Na,K-ATPase activation by insulin appears to be mediated by PKC and PP1 or PP2A.

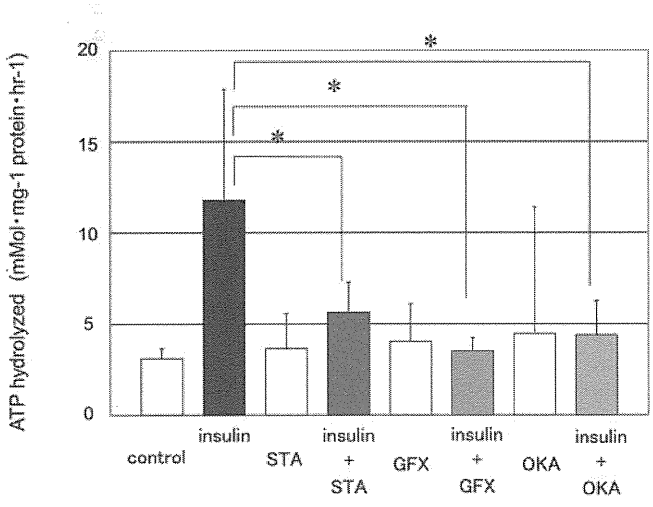

FIGURE 5. Effect of staurosporine (STA), GF109203X (GFX), and okadaic acid (OKA) on insulin-induced Na,K-ATPase activity in cultured mouse corneal endothelial cells. Cells were incubated first for 30 minutes in the absence or presence of 1 μM staurosporine, 0.1 μM GF109203X, or 1 μM okadaic acid and then for an additional 6 hours in the additional presence of 0.1 μM insulin before measurement of Na,K-ATPase activity. Data are mean ± SD of values of four replicates from four representative experiments. $^*P < 0.01$ versus the value for cells incubated with insulin alone (Student's *t*-test). Na,K-ATPase activity did not significantly increase in the presence of staurosporine + insulin, GF109203X + insulin, or okadaic acid + insulin compared with control.

Na,K-ATPase is the largest protein complex in the family of P-type cation pumps, and its minimum functional unit is a heterodimer of the α- and β-subunits.[51] In the case of Na,K-ATPase α-subunits, four isoforms (α_1, α_2, α_3, α_4) are present in mammalian cells.[52] The α_2 isoform appears to be involved in regulating Ca^{2+} transients involved in muscle contraction, whereas the α_1 isoform probably plays a more generalized role.[52] Huang et al.[53] reported that both the α_1 and the α_3 isoforms are expressed in human corneal endothelial cells. We examined Na,K-ATPase α_1-subunit expression in corneal endothelial cells because of its generality. It remains to be investigated whether other isoforms play any role in corneal endothelial cells.

The anti-phospho-Na/K ATPase α_1 antibody we used in the present study recognizes the Na,K-ATPase α_1-subunit only when phosphorylated at Ser18. This phosphorylation triggers endocytosis of the Na,K-ATPase α_1-subunit and results in inhibition of the Na,K-ATPase activity.[48,49] The phospho-Na,K-ATPase α_1-subunit (Ser18) could be regarded as an inactive state of the Na,K-ATPase α_1-subunit. Ser18 itself may be phos-

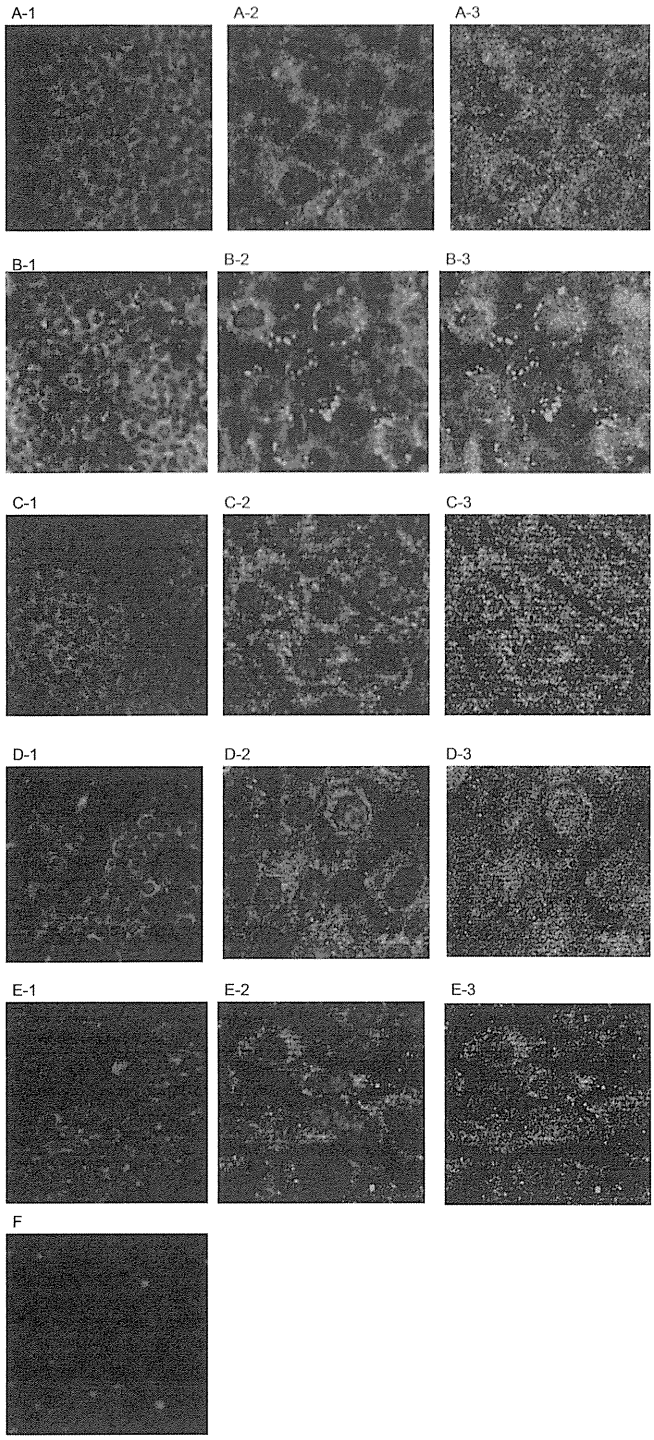

FIGURE 6. Effect of insulin on Na,K ATPase α_1-subunit cell surface expression. Cells were incubated in the absence of insulin (**A**), presence of 0.1 μM insulin for 6 hours (**B**), 0.1 μM insulin for 6 hours with 30 minutes preincubation of 1 μM staurosporine (**C**), 0.1 μM GF109203X (**D**), or 1 μM okadaic acid (**E**) and then were assayed for the cell surface expression of Na,K-ATPase α_1-subunit by immunocytochemistry. (**A-1–E-1**) Low magnification. (**A-2–E-2**) High magnification. (**A-3–E-3**) Without nuclear staining. (**F**) Negative control by using goat anti rabbit IgG (final concentration 2 μg/mL) as a primary antibody.

phorylated directly by PKC.[54–56] In our study, although insulin increased PKC activity, insulin decreased the ratio of phospho-Na,K-ATPase α_1-subunit expression to total Na,K-ATPase α_1-subunit expression. As we previously reported, PKC exerts bidirectional (stimulatory and inhibitory) regulation of Na,K-ATPase activity in mouse corneal endothelial cells, and PKC stimulates Na,K-ATPase activity by activating PP1, PP2A, or both, which dephosphorylates the Na,K-ATPase α_1-subunit in corneal endothelial cells.[57] We also reported that PKC has an inhibitory effect on Na,K-ATPase activity,[57] and this effect may be attributed to Ser18 direct phosphorylation by PKC. In the present study, PDBu phosphorylated the Na,K-ATPase α_1-subunit at 30 minutes; phosphorylation was decreased at 6 hours. The time-response curve of Na,K-ATPase activity by insulin (Fig. 1A) seemed to rise at 2 hours, and the effect became significant at 6 hours and 12 hours. There appears to be a time lag between PKC activation and Na,K-ATPase activation. Some time may be required for subsequent dephosphorylation and cell surface expression of Na,K-ATPase, and it may support our idea that PP1 or PP2A is subsequently activated by insulin-induced PKC. In addition, PP1- and PP2A-induced dephosphorylation of Na,K-ATPase may overcome direct phosphorylation by PKC in corneal endothelial cells. Previous reports also have shown that insulin activates phosphatidylinositol 3-kinase (PI-3 kinase) by insulin/IGF-I receptor, and that PI-3 kinase, presumably acting through PKC, subsequently activates PP1, PP2A, or both in porcine endometrial epithelial cells,[29] rat skeletal muscle cells,[58–60] and frog skin.[61] PP1 or PP2A subsequently dephosphorylates the α-subunit of Na,K-ATPase and stimulates its enzymatic activity.[29,58–60] Ser18 is one of the phosphorylation sites of Na,K-ATPase. Other phosphorylation mechanisms, such as Ser11 dephosphorylation and Tyr10 phosphorylation, may also play roles in Na,K-ATPase activation.[62–64] We selected Ser18 dephosphorylation to prove that dephosphorylation by protein phosphatase 1 or 2A affects Na,K-ATPase activity. Although we did not examine the effect of protein phosphatases on Tyr10 phosphorylation, activation phosphatases should be synergistic and may not prevent the increase in activity by insulin. In the immunocytochemistry phase, insulin increased cell surface expression of the Na,K-ATPase α_1-subunit, and the presence of inhibitors such as staurosporine, okadaic acid, and GF109203X decreased its expression. These results support our conclusions.

Although we did not measure the activity of other kinases, such as SGK or AKT/protein kinase B (PKB), in corneal endothelial cells, recent studies have reported that SGK also activates Na,K-ATPase by increasing the availability of the enzyme at the basolateral membrane and that SGK is under the control of insulin.[35–37] AKT/PKB has been reported to be activated by insulin-induced PI-3 kinase phosphorylation.[65] The ouabain-induced PI-3 kinase-AKT/PKB signaling pathway has been reported to upregulate Na,K-ATPase expression in rat cardiac myocytes[66] and pig kidney epithelial cells,[67] but whether the insulin-induced PI-3 kinase-AKT/PKB pathway activates Na,K-ATPase in corneal endothelium remains unknown. In our study, PKC inhibitors and the PP1/PP2A inhibitor significantly reduced the insulin-induced activation of Na,K-ATPase. This result suggests insulin-induced PKC and PP1/PP2A activation has a significant effect on Na,K-ATPase activation in corneal endothelial cells. However, a slight but insignificant difference existed between the inhibitory effects of PKC inhibitors and the PP1/PP2A inhibitor. In addition, for significant increases, differences in concentrations were seen between PKC activation and Na,K-ATPase activation by insulin, although each similarly reached a plateau at >0.1 μM insulin concentration. In corneal endothelial cells, PP1, PP2A, or both may be activated primarily by insulin-induced PKC activation, whereas the existence of other insulin-induced kinases such as SGK and AKT/PKB must be clarified in further studies. Thus, the mechanism of insulin action is complex, and further studies are necessary to elucidate the pathways by which the effect of insulin on corneal endothelial cells is mediated.

In conclusion, we have shown that insulin increases Na,K-ATPase activity and pump function in corneal endothelial cells. Furthermore, our results support a model in which PKC and PP1 or PP2A mediates the activation of Na,K-ATPase by insulin in corneal endothelial cells. A lack of insulin in type 1 diabetes mellitus or a reduced level of insulin signaling by insulin resistance in type 2 diabetes mellitus may play a role in the pathogenesis of corneal abnormalities in diabetes.

References

1. Brightbill FS, Meyers FL, Brensnick GH. Post-vitrectomy keratopathy. *Am J Ophthalmol.* 1978;85:651-655.
2. Foulks GN, Thoft RA, Perry HD, et al. Factors related to corneal epithelial complications after closed vitrectomy in diabetics. *Arch Ophthalmol.* 1979;97:1076-1079.
3. Perry HD, Foulks GN, Thoft RA, et al. Corneal complications after closed vitrectomy through the pars plana. *Arch Ophthalmol.* 1980; 96:1401-1403.
4. Mandelcorm MS, Blankenship G, Machemer R. Pars plana vitrectomy for the management of severe diabetic retinopathy. *Am J Ophthalmol.* 1976;81:561-570.
5. Schultz RO, Van Horn D, Peters MA, et al. Diabetic keratopathy. *Trans Am Ophthalmol Soc.* 1981;79:180-198.
6. Rao GN, Aquavella JV, Goldberg SH, et al. Pseudophakic bullous keratopathy: relationships to preoperative endothelial status. *Ophthalmology.* 1984;91:1135-1140.
7. Rao GN, Shaw EL, Arther EJ, et al. Endothelial cell morphology and corneal deturgescence. *Ann Ophthalmol.* 1978;11:885-899.
8. O'Niel MR, Polse KA. Decreased endothelial pump function with aging. *Invest Ophthalmol Vis Sci.* 1986;27:457-463.
9. Schultz RO, Matsuda M, Yee RW, et al. Corneal endothelial changes in type 1 and type 2 diabetes mellitus. *Am J Ophthalmol.* 1984;98:401-410.
10. Kim EK, Geroski DH, Holley GP, et al. Corneal endothelial cytoskeletal changes in F-actin with aging, diabetes, and after cytochalasin exposure. *Am J Ophthalmol.* 1992;114:331-335.
11. Roszkowska AM, Tringali CG, Colosi P, et al. Corneal endothelium evaluation in type 1 and type 2 diabetes mellitus. *Ophthalmologica.* 1999;213:258-261.
12. Inoue K, Kato S, Inoue Y, et al. Corneal endothelium and thickness in type 2 diabetes mellitus. *Jpn J Ophthalmol.* 2002;46:65-69.
13. Take G, Karabay G, Erdogan D, et al. The ultrastructural alterations in rat corneas with experimentally-induced diabetes mellitus. *Saudi Med J.* 2006;27:1650-1655.
14. Busted N, Olsen T, Schmitz O. Clinical observations on the corneal thickness and the corneal endothelium in diabetes mellitus. *Br J Ophthalmol.* 1981;65:687-690.
15. Olsen T, Busted N. Corneal thickness in eyes with diabetic and nondiabetic neovascularisation. *Br J Ophthalmol.* 1981;65:691-693.
16. Weston BC, Bourne WM, Polse KA, et al. Corneal hydration control in diabetes mellitus. *Invest Ophthalmol Vis Sci.* 1995;36:586-595.
17. Pierro L, Brancato R, Zaganelli E. Correlation of corneal thickness with blood glucose control in diabetes mellitus. *Acta Ophthalmol (Copenh).* 1993;71:169-172.
18. Skaff A, Cullen AP, Doughty MJ, et al. Corneal swelling and recovery following wear of thick hydrogel contact lenses in insulin-dependent diabetics. *Ophthalmol Physiol Opt.* 1995;15:287-297.
19. Saini JS, Mittal S. In vivo assessment of corneal endothelial function in diabetes mellitus. *Arch Ophthalmol.* 1996;114:649-653.
20. Nishida T. Cornea. In: Krachmer JH, Mannis MJ, Holland EJ, eds. *Cornea.* 2nd ed. London: Elsevier Mosby;2005:3-26.
21. Herse PR. Corneal hydration control in normal and alloxan-induced diabetic rabbits. *Invest Ophthalmol Vis Sci.* 1990;31:2205-2213.
22. Herse PR, Adams L. Effect of hyperglycemia duration on rabbit corneal thickness and endothelial ATPase activity. *Acta Ophthalmol Scand.* 1995;73:158-161.
23. Whikehart DR. The inhibition of sodium, potassium-stimulated ATPase and corneal swelling: the role played by polyols. *J Am Optom Assoc.* 1995;66:331-333.
24. McNamara NA, Brand RJ, Polse KA, et al. Corneal function during normal and high serum glucose levels in diabetes. *Invest Ophthalmol Vis Sci.* 1998;39:3-17.
25. Häring HU, Mehnert H. Pathogenesis of type 2 (non-insulin-dependent) diabetes mellitus: candidates for a signal transmitter defect causing insulin resistance of the skeletal muscle. *Diabetologia.* 1993;36:176-182.
26. Fröjdö S, Vidal H, Pirola L. Alterations of insulin signaling in type 2 diabetes: a review of the current evidence from humans. *Biochim Biophys Acta.* 2009;1792:83-92.
27. Ewart HS, Klip A. Hormonal regulation of the Na^+,K^+-ATPase: mechanisms underlying rapid and sustained changes in pump activity. *Am J Physiol.* 1995;269:C295-C311.
28. Feraille E, Carranza ML, Rousselot M, Favre H. Insulin enhances sodium sensitivity of Na^+,K^+-ATPase in isolated rat proximal convoluted tubule. *Am J Physiol.* 1994;267:F55-F62.
29. Deachapunya C, Palmer-Densmore M, O'Grady SM. Insulin stimulates transepithelial sodium transport by activation of a protein phosphatase that increases Na-K ATPase activity in endometrial epithelial cells. *J Gen Physiol.* 1999;114:561-574.
30. Siegel B, Civan MM. Aldosterone and insulin effects on driving force of Na^+ pump in toad bladder. *Am J Physiol.* 1976;230:1603-1608.
31. Walker TC, Fidelman ML, Watlington CO, Biber TU. Insulin decreases apical membrane resistance in cultured kidney cells (A6). *Biochem Biophys Res Commun.* 1984;124:614-618.
32. Blazer-Yost BL, Cox M, Furlanetto J. Insulin and IGF-I receptor-mediated Na^+ transport in toad urinary bladders. *Am J Physiol.* 1989;257:C612-C620.
33. McGill DL, Guidotti G. Insulin stimulates both the α-1 and the α-2 isoforms of the rat adipocyte (Na+,K+) ATPase. *J Biol Chem.* 1991;266:15824-15831.
34. Erlij D, De Smet P, Van Driessche W. Effect of insulin on area and Na^+ channel density of apical membrane of cultured toad kidney cells. *J Physiol.* 1994;481:533-542.
35. Henke G, Setiawan I, Bohmer C, Lang F. Activation of Na^+/K^+-ATPase by the serum and glucocorticoid-dependent kinase isoforms. *Kidney Blood Press.* 2002;25:370-374.
36. Park J, Leong ML, Buse P, et al. Serum and glucocorticoid-inducible kinase (SGK) is a target of the PI 3-kinase-stimulated signaling pathway. *EMBO J.* 1999;18:3024-3033.
37. Verry F, Summa V, Heitzmann D, et al. Short-term aldosterone action on Na,K-ATPase surface expression: role of aldosterone-induced SGK1? *Ann N Y Acad Sci.* 2003;986:554-561.
38. Coulter JB 3rd, Engelke JA, Eaton DK. Insulin concentration in aqueous humor after paracentesis and feeding of rabbits. *Invest Ophthalmol Vis Sci.* 1980;19:1524-1526.
39. Coulter JB 3rd, Engelke JA, Eaton DK. Insulin concentration in aqueous humor of rabbits: effects of alloxan-diabetes and insulin treatment. *Exp Eye Res.* 1983;37:153-157.
40. Anderson EI, Fischbarg J. Biphasic effects of insulin and ouabain on fluid transport across rabbit corneal endothelium. *J Physiol.* 1978; 275:377-389.
41. Feldman ST, Gately D, Seely BL, Schonthal A, Feramisco JR. Stimulation of DNA synthesis and c-fos expression in corneal endothelium by insulin or insulin-like growth factor-I. *Invest Ophthalmol Vis Sci.* 1993;34:2105-2111.
42. Choi SH, Kay EP, Oh DS, et al. Insulin-like growth factor-I promotes cell proliferation in the absence of modulation of collagen phenotypes and utilizes IRS-1, not PLC-gamma 1, in corneal endothelial cells. *Curr Eye Res.* 1995;14:669-676.
43. Beltowski J, Marciniak A, Jamroz-Wisniewska A, et al. Bidirectional regulation of renal cortical Na^+,K^+-ATPase by protein kinase C. *Acta Biochim Polonica.* 2004;51:757-772.
44. Delamere NA, Parkerson J, Hou Y. Indomethacin alters the Na,K-ATPase response to protein kinase C activation in cultured rabbit nonpigmented ciliary epithelium. *Invest Ophthalmol Vis Sci.* 1997;38:866-875.
45. Lowry OH, Rosebrough NI, Farr AL, Randall RJ. Protein measurement with the Folin phenol reagent. *J Biol Chem.* 1951;193:265-275.

46. Wigham CG, Turner HC, Swan J, Hodson SA. Modulation of corneal endothelial hydration control mechanisms by Rolipram. *Pflugers Arch-Eur J Physiol.* 2000;440:866–870.
47. Mimura T, Yamagami S, Yokoo S, et al. Cultured human corneal endothelial cell transplantation with a collagen sheet in a rabbit model. *Invest Ophthalmol Vis Sci.* 2004;45:2992–2997.
48. Chibalin AV, Ogimoto G, Pedemonte CH, et al. Dopamine-induced endocytosis of Na^+,K^+-ATPase is initiated by phosphorylation of Ser18 in the rat α_1 subunit and is responsible for the decreased activity in epithelial cells. *J Biol Chem.* 1999;274:1920–1927.
49. Yudowski GA, Efendiev R, Pedemonte CH, et al. Phosphoinositide-3 kinase binds to a proline-rich motif in the Na^+,K^+-ATPase α_1 subunit and regulates its trafficking. *Proc Natl Acad Sci U S A.* 2000;97:6556–6561.
50. Feiz V. Corneal edema. In: Krachmer JH, Mannis MJ, Holland EJ, eds. *Cornea.* 2nd ed. London: Elsevier Mosby; 2005:359–363.
51. Jorgensen PL, Hakansson KO, Karlish SJ. Structure and mechanism of Na,K-ATPase: functional sites and their interactions. *Annu Rev Physiol.* 2003;65:817–849.
52. Lingrel J, Moseley A, Dostanic I, et al. Functional roles of the alpha isoforms of the Na,K-ATPase. *Ann N Y Acad Sci.* 2003;986:354–359.
53. Huang B, Blanco G, Mercer RW, et al. Human corneal endothelial cell expression of Na^+,K^+-adenosine triphosphatase isoforms. *Arch Ophhtalmol.* 2003;121:840–845.
54. Feschenko MS, Sweadner KJ. Conformation-dependent phosphorylation of Na,K-ATPase by protein kinase A and protein kinase C. *J Biol Chem.* 1994;269:30436–30444.
55. Feschenko MS, Sweadner KJ. Structual basis for species-specific differences in the phosphorylation of Na,K-ATPase by protein kinase C. *J Biol Chem.* 1995;270:14072–14077.
56. Feschenko MS, Stevenson E, Sweadner KJ. Interaction of protein kinase C and cAMP-dependent pathways in the phosphorylation of the Na,K-ATPase. *J Biol Chem.* 2000;275:34693–34700.
57. Hatou S, Yamada M, Mochizuki H, et al. Role of protein kinase C in regulation of Na^+- and K^+-dependent ATPase activity and pump function in corneal endothelial cells. *Jpn J Ophthalmol.* 2009;53:235–242.
58. Ragolia L, Cherpalis B, Srinivasan M, et al. Role of serine/threonine protein phosphatases in insulin regulation of Na^+/K^+-ATPase activity in cultured rat skeletal muscle cells. *J Biol Chem.* 1997;272:23653–23658.
59. Srinivasan M, Begum N. Stimulation of protein phosphatase-1 activity by phorbol esters: evaluation of the regulatory role of protein kinase C in insulin action. *J Biol Chem.* 1994;269:16662–16667.
60. Srinivasan M, Begum N. Regulation of protein phosphatase 1 and 2A activities by insulin during myogenesis in rat skeletal muscle cells in culture. *J Biol Chem.* 1994;269:12514–12520.
61. Civan MM, Peterson-Yantorno K, O'Brien TG. Insulin and phorbol ester stimulate conductive Na^+ transport through a common pathway. *Proc Natl Acad Sci U S A.* 1988;85:963–967.
62. Efendiev R, Pedemonte CH. Contrary to rat-type, human-type Na,K-ATPase is phosphorylated at the same amino acid by hormones that produce opposite effects on enzyme activity. *J Am Soc Nephrol.* 2006;17:31–38.
63. Feraille E, Carranza ML, Gonin S, et al. Insulin-induced stimulation of Na+, K+-ATPase activity in kidney proximal tubule cells depends on phosphorylation of the α-subunit at Tyr-10. *Mol Biol Cell.* 1999;10:2847–2859.
64. Al-Khalili L, Kotova O, Tsuchida H, et al. ERK1/2 mediates insulin stimulation of Na,K-ATPase by phosphorylation of the α-subunit in human skeletal muscle cells. *J Biol Chem.* 2004;279:25211–25218.
65. Cho JY, Park J. Contribution of natural inhibitors to the understanding of the PI3K/PDK1/PKB pathway in the insulin-mediated intracellular signaling cascade. *Int J Mol Sci.* 2008;9:2217–2230.
66. Liu L, Zhao X, Pierre V, et al. Association of PI3K-Akt signaling pathway with digitalis-induced hypertrophy of cardiac myocytes. *Am J Physiol Cell Physiol.* 2007;293:1489–1497.
67. Tian J, Li X, Liang M, et al. Changes in sodium pump expression dictate the effects of ouabain on cell growth. *J Biol Chem.* 2009;29;284:14921–14929.

Comparison of Anterior and Posterior Corneal Surface Irregularity in Descemet Stripping Automated Endothelial Keratoplasty and Penetrating Keratoplasty

Takefumi Yamaguchi, MD,† Kazuno Negishi, MD,* Kazuko Yamaguchi, MD,* Murat Dogru, MD,*‡ Yuichi Uchino, MD,* Shigeto Shimmura, MD,* and Kazuo Tsubota, MD**

Purpose: To evaluate the irregularity of the anterior and posterior cornea after Descemet stripping automated endothelial keratoplasty (DSAEK) and penetrating keratoplasty (PK).

Methods: This clinical study comprised 39 eyes: 13 consecutive eyes after DSAEK, 13 consecutive eyes after PK, and 13 age-matched normal eyes. Corneal elevation data were acquired using a rotating Scheimpflug camera 1 and 3 months after DSAEK and PK. Anterior and posterior corneal elevation data were decomposed into a set of Zernike polynomials up to eighth order. Total higher-order root mean square (RMS) and RMS from third to eighth order were calculated. The astigmatism and irregularity of the anterior and posterior surfaces were compared between DSAEK and PK.

Results: The regular astigmatism and tilt components of the anterior surface were significantly lower after DSAEK than after PK at 1 and 3 months ($P < 0.001$), whereas there was no difference in astigmatism of the posterior surface between the groups ($P = 0.07$, 0.22). The higher-order RMS and RMSs of third- to eighth-order components of the anterior surface were significantly larger after PK than those after DSAEK at 1 and 3 months ($P < 0.01$), whereas there were no significant differences between DSAEK and PK in higher-order aberration RMS and RMSs of third- to eighth-order components of the posterior surface.

Conclusions: Postoperative corneal irregularity of the anterior surface was greater after PK than after DSAEK, whereas there was no significant difference in posterior surface irregularity. DSAEK is superior to PK in terms of the higher-order irregularity of the anterior surface.

Key Words: DSAEK, penetrating keratoplasty, astigmatism, irregular astigmatism, anterior corneal surface, posterior corneal surface

(*Cornea* 2010;29:1086–1090)

Descemet stripping automated endothelial keratoplasty (DSAEK) for the treatment of dysfunctional endothelium has several advantages over standard penetrating keratoplasty (PK).[1–5] By removing only Descemet membrane and endothelium and retaining the healthy portions of the patients' cornea, DSAEK offers rapid visual recovery and preservation of the corneal biomechanical properties and integrity. Whereas DSAEK is an excellent selective transplantation that has improved the postoperative visual prognosis in patients with bullous keratopathy, it is reported that the majority gain 20/40 vision, but a few gain 20/20 vision. Interface scatter and age are possible factors that affect postoperative visual acuity.[6] In our previous report, the anterior surface irregularity after DSAEK, not the irregularity of the posterior surface, has an important effect on visual acuity,[7] which indicates that, in addition to the corneal transparency, regularity of the anterior surface is an important factor for visual acuity after DSAEK. Postoperative irregularity of the anterior and posterior surfaces must be one of the important factors in selection of DSAEK or PK for the treatment of bullous keratopathy. However, there has been no reported comparison of irregularity between DSAEK and PK. Therefore, we compared the irregularity of anterior and posterior surfaces after DSAEK and PK.

MATERIALS AND METHODS

This study included 39 eyes, 13 age-matched normal eyes without apparent corneal disease and 26 eyes of consecutive patients who underwent DSAEK (13 eyes) and PK (13 eyes) at Keio University Hospital. This retrospective study was approved by the Institutional Review Board of Keio University Hospital. Written informed consent was obtained from all patients. This study adhered to the tenets of the Declaration of Helsinki.

The pre- and postoperative clinical data are shown in Table 1. The average age was 73.7 ± 7.8 years (from 59 to 85 years old; 7 women and 6 men) in the DSAEK group and 62.5 ± 33.5 years (from 31 to 86 years old; 4 women and 9 men) in the PK group. There were no significant differences in age between the groups. The average age of normal patients

Received for publication October 9, 2009; revision received December 4, 2009; accepted December 9, 2009.

From the *Department of Ophthalmology, Keio University School of Medicine, Tokyo, Japan; †Department of Ophthalmology, Tokyo Dental College, Chiba, Japan; and ‡J&J Ocular Surface and Visual Optics Department, Keio University School of Medicine, Tokyo, Japan.

The authors have no proprietary interest in any of the devices mentioned in the article.

Reprints: Takefumi Yamaguchi, Department of Ophthalmology, Keio University School of Medicine, Shinanomachi 35, Shinjuku-ku, Tokyo 1608513, Japan (e-mail: yama19770614@hotmail.com).

TABLE 1. Patients' Data

	DSAEK Group (n = 13)	PK Group (n = 13)	*P*
Age (yrs)	73.7 ± 7.8	62.5 ± 33.5	0.350
Sex			
Female	7	4	
Male	5	9	
Preoperative			
BCVA (logMAR)	1.15 ± 0.49	1.03 ± 0.58	0.289
Spherical equivalent (D)	−1.7 ± 2.1	−2.7 ± 3.1	0.238
Astigmatism (D)	−2.5 ± 1.1	−3.5 ± 2.7	0.072
Postoperative (1 mo)			
BCVA (logMAR)	0.52 ± 0.28	0.58 ± 0.52	0.362
Spherical equivalent (D)	−0.1 ± 1.7	−1.5 ± 2.5	0.052
Astigmatism (D)	−2.3 ± 1.3	−5.5 ± 2.6	<0.001
Corneal thickness (μm)	601 ± 85	562 ± 58	0.10
Postoperative (3 mo)			
BCVA (logMAR)	0.42 ± 0.33	0.49 ± 0.43	0.34
Spherical equivalent (D)	−0.43 ± 2.1	−1.6 ± 2.5	0.11
Astigmatism (D)	−1.9 ± 1.1	−3.7 ± 2.1	<0.001
Corneal thickness (μm)	596 ± 96	529 ± 42	0.019

BCVA, best-corrected visual acuity; D, diopter.

was 65.8 ± 14.4 years (from 35 to 79 years old; 1 man and 12 women). The preoperative logarithm of the minimum angle of resolution (logMAR) was 1.15 ± 0.49 in the DSAEK group and 1.03 ± 0.58 in the PK group.

The causes of bullous keratopathy in the DSAEK group were Fuchs endothelial dystrophy (7 eyes), pseudophakic bullous keratopathy (3 eyes), and bullous keratopathy caused by laser iridotomy (3 eyes). The indications for the PK group included bullous keratopathy (8 eyes), keratoconus (3 eyes), and corneal stromal opacity (2 eyes).

We performed DSAEK according to our standard technique, as previously published. Briefly, after sub-Tenon anesthesia with injection of 2% lidocaine, a 5.0-mm corneoscleral incision was made at the 12-o'clock position. Two paracenteses were made at the 7- and 10-o'clock positions. An anterior chamber maintenance cannula was inserted through the 7-o'clock paracentesis, and Descemet stripping was performed for a diameter of 8.0 mm with a reverse-bent Sinskey hook (Asico, Westmont, IL) corresponding to the 8.0-mm epithelial trephine marker. The recipient's endothelium and Descemet membrane were carefully removed by forceps. Donor precut tissue was obtained from SightLife Eye Bank of Seattle. Precut donors were trephinated at a size of 8.0 mm, and the endothelial surface of the donor lenticle was coated with a small amount of viscoelastic material (Viscoat; Alcon, Fort Worth). Donor tissue was gently folded using forceps and inserted into the anterior chamber. Air was carefully injected into the anterior chamber to unfold the graft. The fluid between the recipient's stroma and the graft was drained from small incisions in the midperipheral recipient cornea. Ten minutes after the air injection, most of the air was replaced with balanced salt solution (Alcon). At the end of the surgery, subconjunctival tobramycin and betamethasone were administered.

PK was performed under retrobulbar anesthesia. The donor button was cut with a Barron punch trephine (diameter, 7.75 mm in all eyes). The recipient bed was 7.5 mm in all cases. A Hessburg–Barron suction trephine was used to cut a partial-depth circular incision in the cornea, centered at the geometric center of the cornea. Excision of the recipient corneal button was completed with curved corneal scissors. The graft was sutured in place with a single-running 10-0 nylon suture with 24 bites. At the end of the surgery, subconjunctival tobramycine and betamethasone were administered.

The corneal topography of the anterior and posterior surfaces was measured using a Pentacam (Oculus, Inc, Wetzlar, Germany). The Pentacam uses a rotating Scheimpflug camera to analyze the anterior segment anatomy. In this study, the Pentacam's 50-picture 3-dimensional scan measurement mode was used. The Pentacam automatically captured images once correct alignment in the x, y, and z directions was attained. After image capture, the instrument analyzed the 50 Scheimpflug images of the anterior eye and allowed export of corneal elevation topographic data (anterior and posterior corneal surfaces). The Pentacam analysis provided data from an area of up to 10 mm in diameter, which included the graft size of 8 mm in this study. Data from the central 4-mm circle were analyzed. No subjects wore contact lenses before and after surgery. The Scheimpflug images were taken 1 and 3 months after DSAEK and PK.

The topographic data of the anterior and posterior surfaces taken by the Pentacam were decomposed into a set of Zernike polynomials. The Zernike coefficients were determined up to eighth order for a 4-mm diameter. The root mean square (RMS) of $Z(2, -2)$ and $Z(2, 2)$ was calculated to represent the lower-order line symmetric component and defined as astigmatism in this study. The RMS of the total higher-order coefficients from third to eighth order was calculated to represent the irregular component of astigmatism and defined as higher-order RMS. We evaluated the postoperative $Z(2, 0)$, astigmatism, RMSs of third to eighth order, and higher-order RMS. The central corneal thickness was measured by the Pentacam. The logarithm of visual acuity was calculated and analyzed statistically. A P value less than 0.05 was considered statistically significant. Comparison of logMAR, corneal thickness, and RMSs of topographic data between DSAEK and PK was performed using Mann–Whitney U test. All statistical analyses were performed with (SAS Institute, Inc, Cary, NC) computer software.

RESULTS

The clinical data are shown in Table 1. The postoperative astigmatism was significantly lower in the DSAEK group than that in the PK group ($P < 0.001$). The postoperative central corneal thickness was significantly larger in the DSAEK group than that in the PK group at 3 months ($P = 0.019$).

Table 2 shows the average of lower-order Zernike coefficients of the anterior surface after DSAEK and PK. In the DSAEK group, although there was a significant difference in astigmatism compared with the normal eye group at 1 month, there were no significant differences in astigmatism and tilt at 3 months. The astigmatism and tilt of the PK group were

TABLE 2. The Average of Lower Order of Zernike Coefficients of Anterior Corneal Surface After DSAEK and PK

	Postoperative (1 Mo)	Postoperative (3 Mo)
DSAEK		
Spherical $Z(2,0)$	150.7 ± 8.3	151.8 ± 8.7
Astigmatism	6.3 ± 4.0†	5.5 ± 4.0
Tilt $Z(11)$	7.1 ± 7.0	5.3 ± 3.3
PK		
Spherical $Z(2,0)$	157.5 ± 19.3	154.7 ± 14.0
Astigmatism	21.7 ± 9.6¶†	16.2 ± 10.1¶†
Tilt $Z(11)$	37.6 ± 19.7¶†	29.3 ± 13.3¶†

Normal eyes (n = 13): spherical $Z(2, 0) = 153.5 \pm 7.1$, astigmatism = 3.3 ± 2.2 D, and tilt $Z(11) = 4.8 \pm 4.4$.

¶$P < 0.05$ compared with the DSAEK group, †$P < 0.05$ compared with the normal eye group.

Mean ± SD (μm).

significantly larger than those of the DSAEK and normal eye groups at 1 and 3 months ($P < 0.05$).

Table 3 shows the average of the lower-order Zernike coefficients of the posterior surface after DSAEK and PK. The spherical component, astigmatism, and tilt of the DSAEK and PK groups were significantly larger than those of the normal eye group at 1 month. There were no differences in spherical aberration, astigmatism, and tilt between the DSAEK and normal eye groups at 3 months. The lower-order Zernike coefficients 3 months after PK were significantly larger than those of the normal eye group.

Table 4 shows the average of the higher-order Zernike coefficients of the anterior surface after DSAEK and PK. The higher-order Zernike coefficients after PK were significantly larger than those after DSAEK and of the normal eye group. There were no significant differences in higher-order Zernike coefficients between the DSAEK and normal eye groups, except for the sixth-order RMS at 1 and 3 months and the eighth-order RMS at 1 month after DSAEK.

Table 5 shows the average of the higher-order Zernike coefficients of the posterior surface after DSAEK and PK. The higher-order Zernike coefficients after DSAEK and PK were significantly larger than those of the normal eye group.

TABLE 3. The Average of Lower Order of Zernike Coefficients of Posterior Corneal Surface After DSAEK and PK

	Postoperative (1 Mo)	Postoperative (3 Mo)
DSAEK		
Spherical $Z(2, 0)$	209.5 ± 20.0†	181.7 ± 31.4
Astigmatism	19.6 ± 5.7†	14.1 ± 7.5
Tilt $Z(11)$	71.7 ± 40.6†	43.8 ± 41.4
PK		
Spherical $Z(2, 0)$	209.3 ± 15.2†	204.0 ± 15.2¶†
Astigmatism	26.4 ± 14.4†	18.9 ± 11.7†
Tilt $Z(11)$	42.9 ± 14.0¶†	45.1 ± 19.8†

Normal eyes (n = 13): spherical $Z(2, 0) = 190.9 \pm 13.7$, astigmatism = 9.5 ± 6.5 D, and tilt $Z(11) = 31.3 \pm 8.4$.

¶$P < 0.05$ compared with the DSAEK group, †$P < 0.05$ compared with the normal eye group.

Mean ± SD (μm).

TABLE 4. The Average of Higher-Order RMS of Zernike Coefficients of Anterior Corneal Surface After DSAEK and PK

	Postoperative (1 Mo)	Postoperative (3 Mo)
DSAEK		
HO-RMS	2.92 ± 2.10	2.54 ± 1.29
S3	2.33 ± 2.06	2.05 ± 1.18
S4	1.50 ± 0.80	1.36 ± 0.64
S5	0.49 ± 0.27	0.43 ± 0.18
S6	0.21 ± 0.14†	0.19 ± 0.10†
S7	0.05 ± 0.06	0.02 ± 0.04
S8	0.01 ± 0.02†	0.00 ± 0.01
PK		
HO-RMS	11.9 ± 5.91¶†	9.86 ± 4.50¶†
S3	10.1 ± 6.03¶†	8.49 ± 4.92¶†
S4	5.28 ± 2.1¶†	4.04 ± 1.08¶†
S5	1.98 ± 1.46¶†	1.71 ± 0.78¶†
S6	0.70 ± 0.65¶†	0.57 ± 0.37¶†
S7	0.26 ± 0.46¶†	0.13 ± 0.13¶†
S8	0.05 ± 0.07¶†	0.04 ± 0.05¶†

Normal eyes (n = 13): HO-RMS = 2.11 ± 0.78, S3 = 1.58 ± 0.67, S4 = 1.23 ± 0.49, S5 = 0.41 ± 0.39, S6 = 0.11 ± 0.07, S7 = 0.02 ± 0.04, and S8 = 0.00 ± 0.00.

¶$P < 0.05$ compared with the DSAEK group, †$P < 0.05$ compared with the normal eye group.

HO-RMS, higher-order RMS.

Mean ± SD (μm).

However, there were no differences in RMSs of the higher-order Zernike coefficients between the DSAEK and PK groups at 1 and 3 months.

DISCUSSION

The important advantage of DSAEK is that it causes little to no change in corneal refractive cylinder compared with PK.[1,8,9] However, the differences in the irregularity of the corneal anterior and posterior surfaces after DSAEK and PK have remained unknown. We reported that the irregularity of the anterior and posterior surfaces decreases after DSAEK, and it is the irregularity of the anterior surface that has an effect on postoperative visual acuity.[7] In this study, we evaluated the difference in the postoperative irregularity of the anterior and posterior surfaces after DSAEK and PK.

Comparing the outcomes of DSAEK and PK, the advantages of DSAEK are rapid visual recovery, lower astigmatism, stability in the postoperative refraction, lower rejection rate, and integrity of the wound structure.[5,9] Hjortdal et al evaluated the efficacy of DSAEK for the treatment of Fuchs endothelial dystrophy and reported that, compared with PK, visual recovery is faster and astigmatism is not induced after DSAEK; however, primary graft failure may be common. In their report, the best-corrected visual acuity at 12 months after DSAEK was significantly better than that after PK.[5] Bahar et al[9] reported that DSAEK enabled rapid and better uncorrected visual acuity and best-corrected visual acuity when compared with PK with significantly lower astigmatism. As for the comparison in regular astigmatism and tilt of the anterior surface between DSAEK and PK, the astigmatism was

TABLE 5. The Average of Higher-Order RMS of Zernike Coefficients of Posterior Corneal Surface After DSAEK and PK

	Postoperative (1 Mo)	Postoperative (3 Mo)
DSAEK		
HO-RMS	17.6 ± 9.2†	11.0 ± 8.56†
S3	14.0 ± 8.68†	8.67 ± 7.67†
S4	9.44 ± 4.20†	5.82 ± 3.96†
S5	3.08 ± 2.03†	1.93 ± 1.69†
S6	1.43 ± 1.17†	0.97 ± 1.09†
S7	0.26 ± 0.19†	0.16 ± 0.15†
S8	0.07 ± 0.06†	0.04 ± 0.09
PK		
HO-RMS	12.0 ± 5.82†	10.7 ± 4.64†
S3	9.79 ± 3.59†	8.24 ± 5.24†
S4	7.13 ± 3.61†	5.41 ± 1.80†
S5	2.92 ± 1.29†	2.31 ± 1.26†
S6	1.27 ± 1.03†	0.90 ± 0.48†
S7	0.27 ± 0.23†	0.25 ± 0.16†
S8	0.10 ± 0.11†	0.10 ± 0.13†

Normal eyes (n = 13): HO-RMS = 3.85 ± 0.95, S3 = 3.13 ± 1.20, S4 = 1.95 ± 0.37, S5 = 0.68 ± 0.32, S6 = 0.23 ± 0.09, S7 = 0.06 ± 0.02, and S8 = 0.02 ± 0.02.

¶$P < 0.05$ compared with the DSAEK group, †$P < 0.05$ compared with the normal eye group.

HO-RMS, higher-order RMS.

Mean ± SD (μm).

significantly lower in DSAEK than in PK, as reported in previous studies,[3,9–11] which seems reasonable because the anterior surface of the cornea is retained in DSAEK. The tilt components of the anterior and posterior surfaces after PK or DSAEK have not been reported previously. We demonstrated that the tilt of the anterior surface in DSAEK was significantly lower than that in PK, although the tilt components of the posterior surface in DSAEK and PK were similar and significantly larger than that in normal eyes. The causes of the tilt component may be eccentric graft preparation, intraoperative decentration of the recipient trephination, and the patients' eye fixation during the examination. It remains unknown whether the corneal tilt component might affect postoperative vision. Manual preparation of the donor and recipient corneas may cause tilt; therefore, keratoplasty using new technology such as femtosecond lasers may make it possible to prepare a precise corneal graft and recipient's corneal cut,[12–18] which may decrease the tilt and other irregular components. Further evaluation of the causes of the postoperative tilt component and its effect on visual acuity is necessary in the future.

In the current study, we demonstrated that the higher-order irregularity of the anterior surface after DSAEK was significantly lower than that after PK, although there was no significant difference in posterior surface between the groups. This is the first report that evaluated the postoperative corneal irregularity of both anterior and posterior surfaces after DSAEK and PK. Terry and Ousley[19] evaluated the topography using TMS and Orbscan after deep lamellar endothelial keratoplasty (DLEK) and reported that DLEK preserves normal corneal topography of the anterior surface and minimizes postoperative astigmatism. McLaren et al[20] evaluated higher-order aberration (HOA) after DLEK and PK and reported that HOAs from the anterior surface were higher after PK than after DLEK. Hindman et al[21] evaluated the light scatter and wavefront aberration after DLEK in 4 patients and reported that the wavefront aberration was lower after DLEK than after PK but that the light scatter because of corneal haze was higher after DLEK than after PK. In our previous report, we demonstrated that the higher-order irregularity of the anterior surface is negatively correlated with postoperative visual acuity.[7] This indicates that, although there are individual differences in anterior surface higher-order irregularity for unknown reasons after DSAEK, its average values were smaller compared with those after PK. In this current study, there was no difference in postoperative logMAR between DSAEK and PK, although the irregularity of the anterior surface was significantly smaller in DSAEK than in PK. The causes of poor visual outcome after DSAEK would be multifactorial: age, light scatter, and irregular astigmatism of the anterior surface as have been reported in the past.[6,7] More comprehensive study on vision-limiting factors measuring corneal opacity, duration of bullous keratopathy, light scatter, and irregular astigmatism after DSAEK and PK should be substantiated in the future.

Evaluation of the corneal posterior surface has been reported by several authors.[2,23] However, the exact level of regular and irregular astigmatism that affects the visual function is unknown. Dubbelman et al[22] reported that the astigmatism of the posterior surface reduces than that of the anterior surface by 31%, which means that the posterior surface has a considerable impact on the total astigmatism. Dubbelman et al[24] calculated the comatic aberration of the whole cornea from a Scheimpflug imaging reconstruction of a normal cornea and concluded that it is sufficient to take only the anterior corneal surface into account because the comatic aberration of the posterior surface is small compared with that of the anterior surface. Sicam et al[23] reported that the spherical aberration of the posterior surface changes with age. Oshika et al[25] reported that the posterior to anterior ratios of the regular and irregular astigmatism are 35.0% ± 41.3% and 39.9% ± 39.9%, respectively, in normal eyes. However, the impact of the posterior corneal surface on vision has not been explained sufficiently, although 2 previous case reports suggested the possible influence of posterior corneal curvature on the visual function.[26,27] Although the irregularity of the posterior surface increased up to the post-PK level after DSAEK in this study, the irregularity of the posterior surface might not affect visual acuity because the small refractive index change between the cornea and aqueous humor is relatively small compared with the change between air and the cornea.

The limit of the current study is that short-term results of postoperative 3 months were examined. Longitudinal studies are needed to follow the long-term alterations in the irregularities of the anterior and posterior surfaces of the cornea after DSAEK and PK. The accuracy of the Pentacam used for the evaluation of the corneal surfaces after DSAEK and PK has not been fully validated. Although the Pentacam, which is a relatively new instrument that images the anterior and posterior corneal surfaces by employing a rotating Scheimpflug camera,

may have some limitations, measurements of corneal thickness and posterior elevation with the Pentacam have been reported to be highly reproducible and repeatable.[28–30] Another limitation of this study is the application of Zernike polynomial functions for the analysis of topographic data of corneal surfaces, not HOA. The validity of Zernike polynomial functions to represent the corneal surface might be a subject that requires more study. Smolek and Klyce[31] evaluated the corneal topography of normal eyes and eyes after PK, radial keratotomy, and keratoconus and reported that the fourth-order Zernike polynomial seemed reliable for modeling the normal cornea and that if more Zernike terms were added, the accuracy of the fit to the abnormal cornea will be improved to the degree of the minimum errors found in normal corneas. We evaluated the corneal surfaces using Zernike polynomials up to eighth order. The eighth-order values after DSAEK and PK were very small or nearly zero, which may indicate the validity of the fit to the abnormal surfaces by eighth-order Zernike polynomials and may sufficiently reflect the true surface values. More comprehensive studies should be performed in future.

In conclusion, the irregularity of the anterior surface was significantly smaller after DSAEK compared with that after PK, whereas there was no significant difference in the posterior surface irregularity. DSAEK is superior to PK in terms of the higher-order irregularity of the anterior surface.

REFERENCES

1. Price MO, Price FW Jr. Descemet's stripping with endothelial keratoplasty: comparative outcomes with microkeratome-dissected and manually dissected donor tissue. *Ophthalmology.* 2006;113:1936–1942.
2. Price FW Jr, Price MO. Descemet's stripping with endothelial keratoplasty in 50 eyes: a refractive neutral corneal transplant. *J Refract Surg.* 2005;21: 339–345.
3. Price MO, Price FW. Descemet's stripping endothelial keratoplasty. *Curr Opin Ophthalmol.* 2007;18:290–294.
4. Koenig SB, Covert DJ. Early results of small-incision Descemet's stripping and automated endothelial keratoplasty. *Ophthalmology.* 2007; 114:221–226.
5. Hjortdal J, Ehlers N. Descemet's stripping automated endothelial keratoplasty and penetrating keratoplasty for Fuchs' endothelial dystrophy. *Acta Ophthalmol.* 2009;87:310–314.
6. Patel SV, Baratz KH, Hodge DO, et al. The effect of corneal light scatter on vision after Descemet stripping with endothelial keratoplasty. *Arch Ophthalmol.* 2009;127:153–160.
7. Yamaguchi T, Negishi K, Yamaguchi K, et al. Effect of anterior and posterior corneal surface irregularity on vision after Descemet-stripping endothelial keratoplasty. *J Cataract Refract Surg.* 2009;35:688–694.
8. Price FW Jr, Price MO. Descemet's stripping with endothelial keratoplasty in 200 eyes: early challenges and techniques to enhance donor adherence. *J Cataract Refract Surg.* 2006;32:411–418.
9. Bahar I, Kaiserman I, McAllum P, et al. Comparison of posterior lamellar keratoplasty techniques to penetrating keratoplasty. *Ophthalmology.* 2008; 115:1525–1533.
10. Terry MA, Shamie N, Chen ES, et al. Precut tissue for Descemet's stripping automated endothelial keratoplasty: vision, astigmatism, and endothelial survival. *Ophthalmology.* 2009;116:248–256.
11. Bahar I, Kaiserman I, Levinger E, et al. Retrospective contralateral study comparing Descemet stripping automated endothelial keratoplasty with penetrating keratoplasty. *Cornea.* 2009;28:485–488.
12. Cheng YY, Pels E, Nuijts RM. Femtosecond-laser-assisted Descemet's stripping endothelial keratoplasty. *J Cataract Refract Surg.* 2007;33: 152–155.
13. Buratto L, Bohm E. The use of the femtosecond laser in penetrating keratoplasty. *Am J Ophthalmol.* 2007;143:737–742.
14. Slade SG. Applications for the femtosecond laser in corneal surgery. *Curr Opin Ophthalmol.* 2007;18:338–341.
15. Farid M, Kim M, Steinert RF. Results of penetrating keratoplasty performed with a femtosecond laser zigzag incision initial report. *Ophthalmology.* 2007;114:2208–2212.
16. Por YM, Cheng JY, Parthasarathy A, et al. Outcomes of femtosecond laser-assisted penetrating keratoplasty. *Am J Ophthalmol.* 2008;145: 772–774.
17. Price FW Jr, Price MO, Grandin JC, et al. Deep anterior lamellar keratoplasty with femtosecond-laser zigzag incisions. *J Cataract Refract Surg.* 2009;35:804–808.
18. Farid M, Steinert RF. Deep anterior lamellar keratoplasty performed with the femtosecond laser zigzag incision for the treatment of stromal corneal pathology and ectatic disease. *J Cataract Refract Surg.* 2009;35:809–813.
19. Terry MA, Ousley PJ. Replacing the endothelium without corneal surface incisions or sutures: the first United States clinical series using the deep lamellar endothelial keratoplasty procedure. *Ophthalmology.* 2003;110: 755–764; discussion 64.
20. McLaren JW, Patel SV, Bourne WM, et al. Corneal wavefront errors 24 months after deep lamellar endothelial keratoplasty and penetrating keratoplasty. *Am J Ophthalmol.* 2009;147:959–965.
21. Hindman HB, McCally RL, Myrowitz E, et al. Evaluation of deep lamellar endothelial keratoplasty surgery using scatterometry and wavefront analyses. *Ophthalmology.* 2007;114:2006–2012.
22. Dubbelman M, Sicam VA, Van der Heijde GL. The shape of the anterior and posterior surface of the aging human cornea. *Vision Res.* 2006;46: 993–1001.
23. Sicam VA, Dubbelman M, van der Heijde RG. Spherical aberration of the anterior and posterior surfaces of the human cornea. *J Opt Soc Am A Opt Image Sci Vis.* 2006;23:544–549.
24. Dubbelman M, Sicam VA, van der Heijde RG. The contribution of the posterior surface to the coma aberration of the human cornea. *J Vis.* 2007; 7:10 1-8.
25. Oshika T, Tomidokoro A, Tsuji H. Regular and irregular refractive powers of the front and back surfaces of the cornea. *Exp Eye Res.* 1998;67:443–447.
26. Rao SK, Padmanabhan P. Posterior keratoconus. An expanded classification scheme based on corneal topography. *Ophthalmology.* 1998;105: 1206–1212.
27. Shimmura S, Yang HY, Bissen-Miyajima H, et al. Posterior corneal protrusion after PRK. *Cornea.* 1997;16:686–688.
28. O'Donnell C, Maldonado-Codina C. Agreement and repeatability of central thickness measurement in normal corneas using ultrasound pachymetry and the OCULUS Pentacam. *Cornea.* 2005;24:920–924.
29. Al-Mezaine HS, Al-Amro SA, Kangave D, et al. Comparison between central corneal thickness measurements by oculus pentacam and ultrasonic pachymetry. *Int Ophthalmol.* 2008;28: 333–338.
30. Ho JD, Tsai CY, Tsai RJ, et al. Validity of the keratometric index: evaluation by the Pentacam rotating Scheimpflug camera. *J Cataract Refract Surg.* 2008;34:137–145.
31. Smolek MK, Klyce SD. Goodness-of-prediction of Zernike polynomial fitting to corneal surfaces. *J Cataract Refract Surg.* 2005;31: 2350–2355.

Ophthalmic Research

Ophthalmic Res 2010;44:145
DOI: 10.1159/000316446

Published online: September 9, 2010

Editorial

The life span in developed countries has been increasing for the last 20 years, and surprisingly this trend is likely to continue its steady increase over the upcoming decades too. The impact of this trend is that the population consists of more elderly people. Since elderly people show a tendency towards age-related eye disorders, modern societies are transferring this major challenge to the ophthalmic community. The major blinding diseases such as cataracts, glaucoma, diabetic retinopathy and age-related macular degeneration are most affected by aging. Even the genetic disorders, such as retinitis pigmentosa, can be considered 'premature aging of the retina' and are affected by aging. Not only the blinding diseases, but also other major diseases such as dry eye or presbyopia, which dramatically affect quality of vision, are affected by aging. Thus, in the aging societies of developed countries, aging is a very important factor in ophthalmology.

Recent advances in the understanding of aging have given us a new way of thinking about the intervention in the aging process. The advances in aging research may be able to provide the chance to interfere with the aging process itself, including that of the eye. One hard evidence comes from calorie restriction (CR) intervention. CR extends the life span in many species. Fortunately CR can also suppress the incidence of age-related diseases such as cancer, diabetes and cardiovascular events, and possibly age-related eye disorders.

In addition to the CR theory, the oxidative stress theory is another important hypothesis that is believed to be involved in aging. According to this theory, we can manage the aging process by controlling reactive oxygen species (ROS). Since the main function of the eye is 'seeing' which is mediated by photoprocessing of the retinal cells, light exposure, especially blue to ultraviolet light, can induce ROS. The production of ROS in the retina is an unavoidable event of normal eye function. Also, the ocular surface is exposed to the ambient environment of which oxygen levels fluctuate with each blink and polluted air. Thus, the ROS theory is also a very important consideration.

In this issue focusing on the antiaging approach for eye disorders, there are reviews based on the CR theory and the oxidative stress theory. The first review by Tsubota et al. for dry eye care is based on the two aforementioned theories. The CR-theory-based reviews in this issue point out the importance of mitochondria (paper by Jarrett et al.) and sirtuins (article by Ozawa and Kubota). These issues provide new challenges and are expected to open a very important field in the near future. The oxidative-stress-theory-based reviews comprise evidence from epidemiological studies (by Fletcher), the importance of nutrition (by Agte and Tarwadi), prevention of age-related cataracts (by Beebe et al.) and glaucoma (by Chrysostomou et al.). These reviews offer new and comprehensive information; thus, the readers can obtain a clear picture on how the oxidative control is important for the prevention and treatment of eye diseases from the point of view of aging.

Antiaging research has recently come of age. The practical approach using the fundamentals of aging research is not used clinically yet; however, ROS control, such as supplementation based on the Age-Related Eye Disease Study, is the beginning of the application of ROS control for the age-related disorders. A proper diet, including CR or antioxidant food factors, antioxidant supplements and exercise may become important interventions for the age-related eye disorders. Future developments may include drug intervention in addition to supplements based on the antiaging approach.

Kazuo Tsubota, Tokyo

KARGER

Fax +41 61 306 12 34
E-Mail karger@karger.ch
www.karger.com

0030–3747/10/0443–0145$26.00/0

Accessible online at:
www.karger.com/ore

Mathematical Projection Model of Visual Loss Due to Fuchs Corneal Dystrophy

Shin Hatou,[1] Shigeto Shimmura,[1] Jun Shimazaki,[2] Tomohiko Usui,[3] Shiro Amano,[3] Hideaki Yokogawa,[4] Akira Kobayashi,[4] Xiaodong Zheng,[5] Atsushi Shiraishi,[5] Yuichi Ohashi,[5] Tsutomu Inatomi,[6] and Kazuo Tsubota[1]

Purpose. To devise a mathematical disease classification model for eyes with primary guttata cornea, on the bases of endothelial loss trajectory and probability of advanced disease.

Methods. A series of 1971 patients (3281 eyes), some with and some without guttata corneas, undergoing specular microscopy were retrospectively reviewed. The eyes were classified into four stages; stage 0, without guttae; 1, guttata cornea without edema; 2, mild Fuchs' corneal dystrophy (FCD); and 3, severe FCD, according to clinical records, and patient age and corneal endothelial cell density (ECD) were plotted. Nonparametric density smoothing was used to create a contour map, and a best-fit curve for ECD loss was calculated. The relation between ECD decrease rate and the stages were evaluated.

Results. Endothelial decrease rate in stage 0 was 0.44%/year, which was compatible with that of normal eyes reported in previous studies. Decrease rates of stages 1, 2, and 3 were 0.81%, 2.65%, and 3.08%/ year, respectively. The age-ECD loss curves of 1.40%/year ($ECO_{1.4}$) and 2.00%/year ($ECO_{2.0}$) further divided stage 1 into three subgroups; stage 1a, asymptomatic guttata cornea; 1b, borderline guttata cornea; and 1c, pre-FCD. The $ECO_{2.0}$ cutoff line differentiated eyes with FCD from those without edema with a sensitivity and specificity of >90%. Stage 1c eyes were below $ECO_{2.0}$ and had a decrease rate as high as FCD.

Conclusions. This mathematical model can be used to predict the prognosis of patients with primary guttata cornea. (*Invest Ophthalmol Vis Sci.* 2011;52:7888-7893) DOI:10.1167/iovs.11-8040

From the [1]Department of Ophthalmology, Keio University School of Medicine, Shinjuku, Japan; the [2]Department of Ophthalmology, Tokyo Dental College Ichikawa General Hospital, Tokyo, Japan; the [3]Department of Ophthalmology, Tokyo University School of Medicine, Tokyo, Japan; the [4]Department of Ophthalmology, Kanazawa University School of Medicine, Kanazawa, Japan. the [5]Department of Ophthalmology, Ehime University School of Medicine, Matsuyama, Japan; and the [6]Department of Ophthalmology, Kyoto Prefectural University of Medicine, Kyoto, Japan.

Supported by a grant from the Ministry of Health, Labor and Welfare, Japan. The sponsor or funding organization had no role in the design or conduct of this research.

Submitted for publication June 14, 2011; revised August 8, 2011; accepted August 12, 2011.

Disclosure: **S. Hatou**, None; **S. Shimmura**, None; **J. Shimazaki**, None; **T. Usui**, None; **S. Amano**, None; **H. Yokogawa**, None; **A. Kobayashi**, None; **X. Zheng**, None; **A. Shiraishi**, None; **Y. Ohashi**, None; **T. Inatomi**, None; **K. Tsubota**, None

Corresponding author: Shigeto Shimmura, Department of Ophthalmology, Keio University School of Medicine, 35 Shinanomachi, Shinjuku, Tokyo 160-8582, Japan;shige@sc.itc.keio.ac.jp.

Fuchs' corneal dystrophy (FCD) is a progressive, bilateral corneal dystrophy.[1] There is a progressive loss of corneal endothelial cells with secretion of an abnormally thickened basement membrane, leading to corneal guttae formation.[1] On specular microscopy, these corneal guttae are observed as dark areas.[1,2] As endothelial function deteriorates, corneal edema increases and visual acuity declines,[2] and FCD is a major indication for keratoplasty (corneal transplants) in the United States.[3-5] Although FCD is recognized as a dominantly inherited disorder, females are predisposed to it and develop corneal guttae 2.5 times more frequently than do males, progressing to corneal edema 5.7 times more often than do males.[6] The prevalence of primary guttata cornea and FCD are lower in Japan than in the United States.[7,8] This difference in prevalence is thought to be mainly attributable to the racial difference.[7]

Primary guttata cornea is believed to be a preliminary stage of FCD. Krachmer et al.[6] graded guttata cornea and FCD according to a spread of guttae and reported that there was a positive correlation between age and grade of guttae. However, the exact natural course of guttata cornea, or whether all cases of guttata cornea progress to FCD remains to be determined. A prospective study that follows the decline in endothelial cells density (ECD) with age would be ideal for predicting the natural course of guttata cornea; however, a very long follow-up would be required, and recruiting asymptomatic potential patients is practically impossible, especially in Japan. A retrospective study with a large database and an adequate mathematical model can be used in a similar way to predict the prognosis of patients with guttata cornea. In this report, we retrospectively reviewed age and ECD in a large group of hospital-based patients and evaluated the prevalence of guttae, male:female ratio, and distribution of age and ECD. In addition, we propose a new classification of guttata cornea based on a mathematical model that adequately predicts the prognosis of disease.

Methods

Subjects

Clinical records of outpatients who underwent specular microscopy for corneal endothelial cell counts from January through December 2009 in six hospitals affiliated with the Fuchs' Corneal Dystrophy Study Group of Japan were retrospectively reviewed. The purpose of specular microscopy for those patients were routine examination before ocular surgery, follow-up for corneal diseases that were thought to have little effect on endothelium (such as keratoconus or lattice corneal dystrophy), or follow-up for diagnosed Fuchs' corneal dystrophy. Patients who had a history of trauma, corneal infection, intraocular inflammation, intraocular surgery, or laser iridotomy were excluded from the study. Endothelial photographs were taken at the center of the pupillary area with a noncontact specular microscope (Nonkon Robo F & A; Konan Medical, Nishinomiya, Japan, or EM-3000; Tomey,

Investigative Ophthalmology & Visual Science, October 2011, Vol. 52, No. 11

Nagoya, Japan), and analyses of the photographs were performed with an automatic cell analysis system attached to the microscope. Data concerning patient age, sex, presence of guttae, and ECD were recorded. The eyes were classified into four groups by slit lamp examination according to modified Stocker's classification[9]:

Stage 1: Guttata cornea without the stroma or the epithelium being affected

Stage 2: Permeation of corneal stroma with fluid, edema of epithelium, and bullae formation

Stage 3: Late stages with subepithelial connective tissue formation, vascularization, and scar formation

Other eyes without corneal guttae were classified as stage 0. During the rest of the article, the term Fuchs' corneal dystrophy (FCD) represents stage 2 and 3, since eyes in these stages have symptoms related to corneal edema. The study complied with the Declaration of Helsinki. Approval was granted by the Committee for the Protection of Human Subjects of each hospital.

Mathematical Model of Endothelial Cell Loss Rate

To construct a mathematical model of decrease in endothelial cells, we made the following two assumptions:

1. The ECD at 5 years of age is 3600 cells/mm^2. This is common to all classes.
2. From 5 years of age, the decrease rate (percent/year) of ECD is constant in each class, but different between classes.

Murphy et al.[10] reported that during first 2 years of life ECD decreased rapidly because of corneal growth, and after that the decrease rate slows down to 0.56%/year. The effect of corneal growth on ECD ends at 5 years of age or earlier. To simplify our mathematical model, we assumed that ECD at 5 years of age was common to all classes and regarded this point as the base point of age-ECD curve in our mathematical model. Because the onset of FCD is in adulthood, we believe that this assumption is acceptable. We substituted the mean ECD of normal 5-year-old children (3600 cells/mm^2) in the report of Nucci et al.[11] for the base point. We assumed that the (percentage) decrease rate is dependent on the class, and it is constant in each class from 5 years of age. Based on these assumptions, the following differential equation stands:

$$dE_{(t)}/d(t) = -(D/100) \cdot E_{(t)}$$

$$E_{(t=0)} = 3600$$

where t is age 5 years; $E_{(t)}$ is endothelial cell density at t years (in cells per square millimeter); and D is the decrease rate (percent).

The solution to the differential equation is the following:

$$E_{(t)} = 3600e^{[-(D/100)t]}$$

Using this mathematical model, an age-ECD curve in each class can be drawn by the least-squares method. An age–ECD curve of optimal decrease rate can be drawn as well.

Statistical Analysis

Scatterplotting, analysis of variance (ANOVA), nonparametric density smoothing, age-ECD curve, and other statistical analyses were calculated by or written in commercial software (Excel 2007; Microsoft, Redmond, WA, and JMP 8 software; SAS, Cary, NC). $P < 0.05$ was considered statistically significant.

Results

Characteristics of Patients

Age, sex, and stage of reviewed patients and eyes are presented in Table 1. The prevalence of guttata cornea (stage 1+2+3) was 12.73%. The prevalence of stage 1 was 10.65%, and FCD (stage 2+3) was 2.08%. The male: female ratio in each stage was as follows; 1: 1.03 (stage 0), 1: 1.88 (stage 1), 1: 2.43 (stage 2), and 1: 4.67 (stage 3). Females were more predisposed to stage 1 or FCD than males, and the ratio increased in advanced stages.

Age-ECD Curve of 2.0% Differentiates Fuchs' Dystrophy

Figure 1, left shows the scatterplot between age and ECD for each stage. Nonparametric density smoothing was drawn on the scatterplot (Fig. 1, right), which represents the contour of plot density. The age-ECD curves based on our mathematical model were drawn by the least-squares method. Table 2 shows ECD with sample sizes at 5-year intervals for grades 0 to 3, which enables the mean ECD data of grade 0 to 3 to be compared at various ages.

The decreased rate curve of stage 1 age-ECD was 0.81%, which was closer to that of stage 0 (decrease rate, 0.44%) than that of stage 2 (2.65%) or stage 3 (3.08%). The decrease rate of stage 0 in our study was 0.44%, which is within the range of

Table 1. The Age, Sex, and Stages of Reviewed Patients and Eyes

Patient Stage	Age, y (Mean ± SD)	Male (*n*)	Female (*n*)	Total (*n*)	Prevalence (%) Total	Male	Female
0	65.3 ± 16.2	848	872	1720			
1	68.5 ± 14.3	73	137	210	10.65	7.84	13.17
2	70.3 ± 10.6	7	17	24	1.22] 2.08	0.75] 1.07	1.63] 2.98
3	75.1 ± 12.4	3	14	17	0.86	0.32	1.35
Total	66.6 ± 15.4	931	1040	1971	12.73	8.91	16.15

Eye Stage	Male (*n*)	Female (*n*)	Total (*n*)
0	1426	1483	2909
1	103	205	308
2	13	28	41
3	5	18	23
Total	1547	1734	3281

Prevalence of FCD was calculated as sum of stage 2 and 3. In this table, if a patient had eyes in different stages, then he or she was classified in the severer of the stages between the eyes.

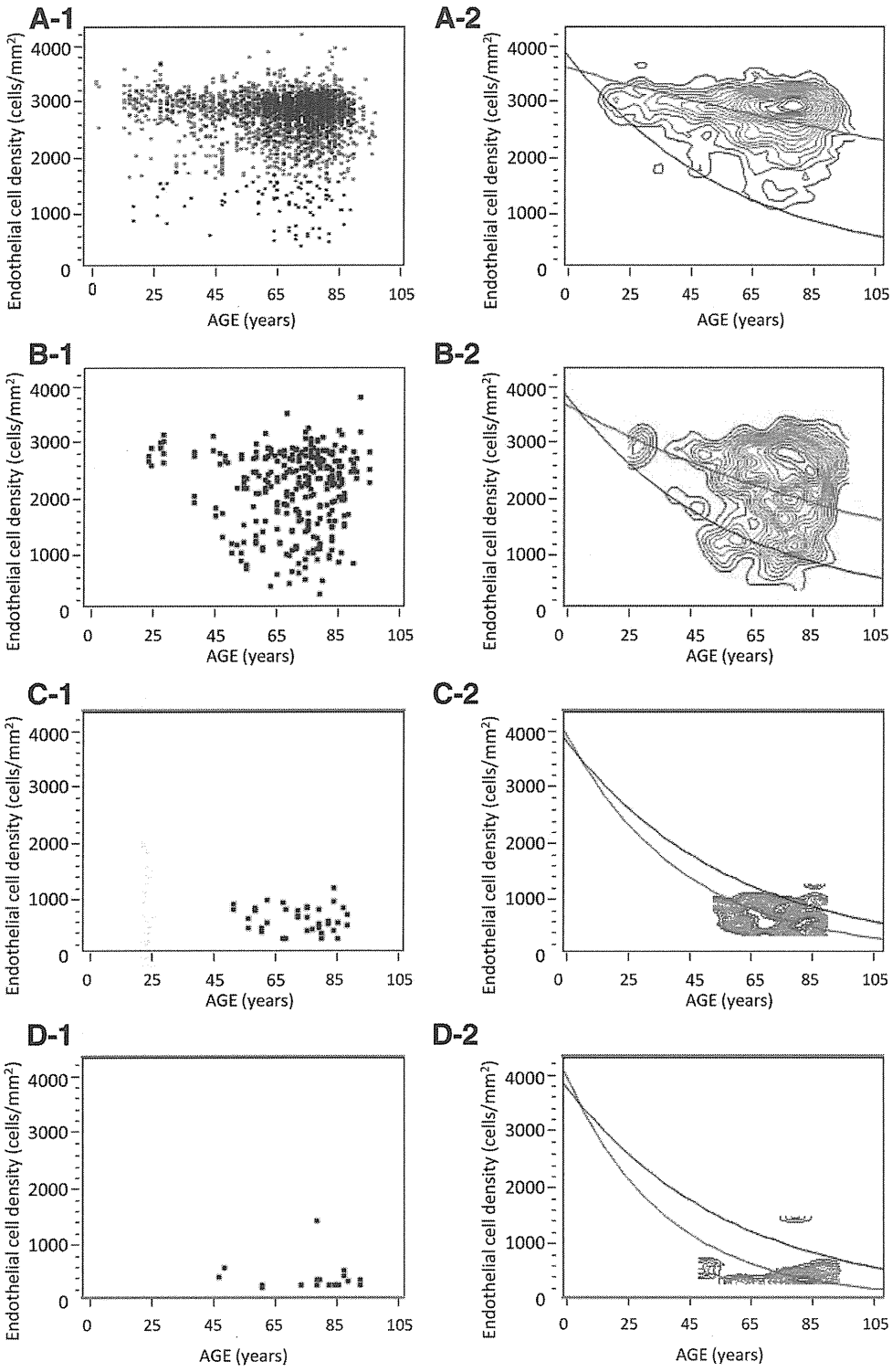

FIGURE 1. Scatterplots (*left*) and contour maps of nonparametric density smoothing (*right*) of each stage. (**A-1**, **A-2**) Stage 0, (**B-1**, **B-2**) stage 1, (**C-1**, **C-2**) stage 2, and (**D-1**, **D-2**) stage 3. *Red curves*: age-ECD curves of each stage calculated by least-squares method. The decrease rates of each stage were 0.44% (stage 0), 0.81% (stage 1), 2.65% (stage 2), and 3.08% (stage 3). The contour maps showed that the age-ECD curve of 2.00% decrease rate ($ECO_{2.0}$, *black curves*) ran through a trough between peaks of all stages. Most of the peaks in stages 0 and 1 were located above $ECO_{2.0}$, whereas peaks of stages 2 and 3 were located below $ECO_{2.0}$.

normal eyes reported in previous studies (Table 3).[10,12–16] Contour maps show that most of the peaks in stage 0 and 1 were located above the age-ECD curve of the 2.00% decrease rate, whereas peaks of stage 2 and 3 were located below this curve. Table 4 shows binary classification based on the age-ECD curve of a 2.00% decrease rate, designated novel ECD cutoff 2 ($ECO_{2.0}$), dividing stages 0+1 and stages 2+3 (Table 4) or stage 1 and stages 2+3 (Table 4). The high sensitivity and specificity of these classifications suggested that $ECO_{2.0}$ is an adequate cutoff between eyes with corneal edema and those without edema.

Age-ECD Curve of 1.4% and 2.0% Divides Stage 1 into Three Distinct Groups

The contour map of stage 1 consisted of several peaks. Figure 2 shows that the age-ECD curve of the 1.40% decrease rate, designated novel ECD-cutoff point 1 ($ECO_{1.4}$), divides these peaks into a high-density group ($>ECO_{1.4}$), and a low-density group ($<ECO_{1.4}$). ANOVA revealed that the age-ECD curves of each group predicted ECD according to age, with statistical significance: The F ratio and P value were 803.3 and <0.0001

TABLE 2. Mean ECD with Sample Sizes at 5-Year Intervals for Grades 0 to 3

	0–9 y		10–14 y		15–19 y		20–24 y		25–29 y	
	Eyes	ECD	Eyes	ECD	Eyes	ECD	Eyes	ECD	Eyes	ECD
Stage 0	4	3073.3 ± 392.6	7	3020.4 ± 330.1	47	2769.2 ± 530.1	31	2837.4 ± 567.3	60	2853.1 ± 507.6
Stage 1	0	—	0	—	0	—	4	2765.0 ± 128.8	6	2954.5 ± 175.6
Stage 2	0	—	0	—	0	—	0	—	0	—
Stage 3	0	—	0	—	0	—	0	—	0	—
	30–34 y		35–39 y		40–44 y		45–49 y		50–54 y	
	Eyes	ECD	Eyes	ECD	Eyes	ECD	Eyes	ECD	Eyes	ECD
Stage 0	58	2732.6 ± 511.3	54	2741.9 ± 324.7	80	2672.2 ± 462.5	99	2687.8 ± 507.8	128	2754.6 ± 370.5
Stage 1	0	—	4	2423.0 ± 474.1	7	2503.7 ± 541.9	7	1934.3 ± 763.9	14	1865.2 ± 703.0
Stage 2	0	—	0	—	0	—	2	881.0 ± 60.8	2	592.0 ± 120.2
Stage 3	0	—	0	—	1	461.0	1	622.0	0	—
	55–59 y		60–64 y		65–69 y		70–74 y		75–79 y	
	Eyes	ECD	Eyes	ECD	Eyes	ECD	Eyes	ECD	Eyes	ECD
Stage 0	195	2701.2 ± 408.1	325	2671.9 ± 464.4	384	2677.7 ± 449.1	494	2698.4 ± 435.0	496	2691.2 ± 421.3
Stage 1	25	2105.2 ± 673.3	28	2219.4 ± 695.5	39	2124.8 ± 743.7	61	2242.5 ± 719.4	44	2159.0 ± 741.7
Stage 2	4	645.8 ± 224.3	2	797.5 ± 282.1	7	562.9 ± 329.5	7	730.7 ± 149.5	7	483.0 ± 183.7
Stage 3	2	284.5 ± 21.9	0	—	0	—	2	302.5 ± 3.5	7	524.0 ± 418.9
	80–84 y		85–89 y		≥90 y					
	Eyes	ECD	Eyes	ECD	Eyes	ECD				
Stage 0	309	2698.9 ± 440.4	116	2624.5 ± 457.3	22	2563.7 ± 299.3				
Stage 1	47	2264.2 ± 556.2	17	2279.2 ± 597.9	5	2962.0 ± 597.1				
Stage 2	7	680.6 ± 318.1	3	723.3 ± 155.7	0	—				
Stage 3	5	302.4 ± 5.4	3	482.3 ± 97.1	2	352.5 ± 74.2				

Eye data are expressed as the number, and the ECD in cells per square millimeter.

in the high-density group and 945.7 and <0.0001 in the low-density group. The decrease rate of the age-ECD curve in the high-density group was 0.56%, which was very close to that of the stage 0 age-ECD curve. On the other hand, the decrease rate in the low-density group was 2.00%, which coincided with $ECO_{2.0}$. These results suggest that the decrease rate of the high-density group in stage 1 was nearly normal, whereas the low-density group in stage 1 was located on the border between eyes with and without corneal edema. We therefore classified stage 1 on the basis of $ECO_{1.4}$ and $ECO_{2.0}$, as follows (Fig. 3):

Stage 1a, asymptomatic guttata cornea (AGC): above $ECO_{1.4}$

Stage 1b, borderline guttata cornea (BGC): between $ECO_{1.4}$ and $ECO_{2.0}$

Stage 1c, preliminary stage of FCD (pre-FCD): below $ECO_{2.0}$

TABLE 3. Decrease Rates of Stage 0 in the Present Study and Normal Unoperated Eyes Reported in the Previous Studies

Author	Decrease Rate (%/y)	Nation
Murphy et al.[10]	0.56	United States
Cheng et al.[12]	1.00	England
Ambrose et al.[13]	0.60	England
Numa et al.[14]	0.30	Japan
Bourne et al.[15]	0.60	United States
Rao et al.[16]	0.30	India
Present study	0.44	Japan

DISCUSSION

To obtain a sufficient number of age-ECD data to compare FCD (stage 2+3), guttata cornea without edema (stage 1), and control group without guttata cornea (stage 0), we performed a retro-

TABLE 4. Binary Classification of Clinical Stage

Clinical Stage	Classification Based On $ECO_{2.0}$		
	Below $ECO_{2.0}$	Above $ECO_{2.0}$	Total
Total Eyes			
Stage 2+3	60	4	64
Stage 0+1	122	3095	3217
Total	182	3099	3281
Sensitivity, %	93.75		
Specificity, %	96.21		
Eyes with Guttata Cornea			
Stage 2+3	60	4	64
Stage 1	27	281	308
Total	87	285	372
Sensitivity, %	93.75		
Specificity, %	91.23		

Data are based on the age-ECD curve of 2.00% decrease rate as a novel ECD-cut-off ($ECO_{2.0}$), sensitivity and specificity to detect stage 2+3 from total eyes or the eyes with guttata cornea based on the classification.

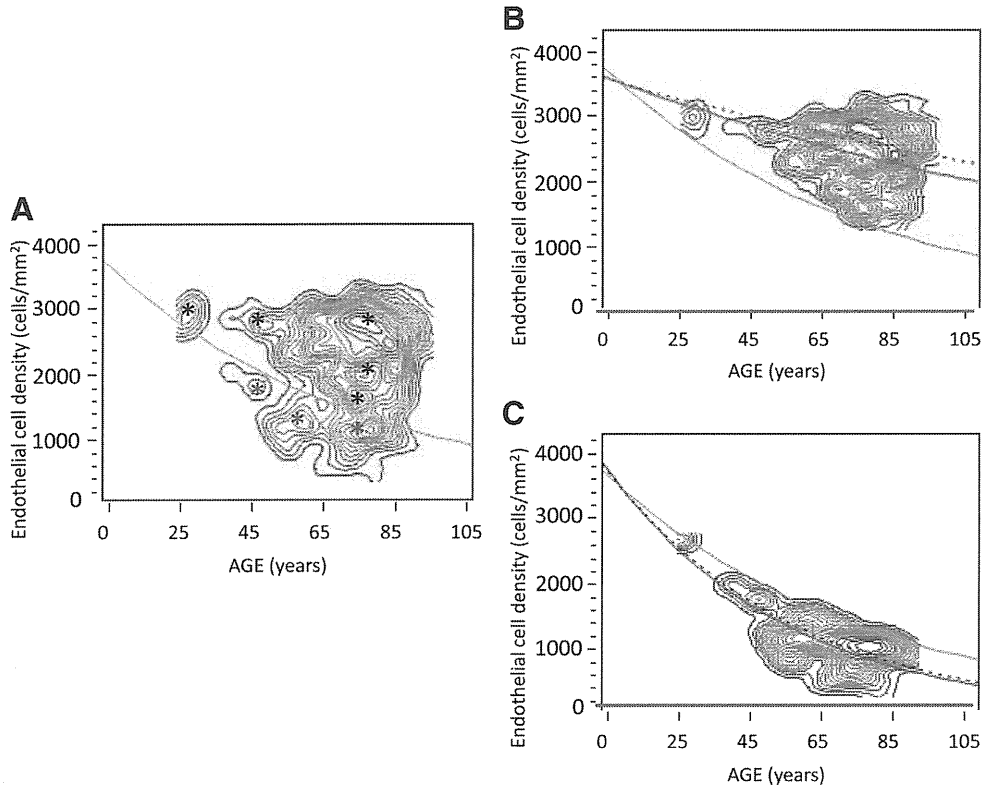

FIGURE 2. (**A**) The contour map of nonparametric density smoothing in stage 1. Stage 1 consisted of several peaks, and the age-ECD curve of 1.40% decrease rate ($ECO_{1.4}$, *green curve*) ran through a trough between peaks of high ECD group (*black asterisks*) and low ECD group (*red asterisks*). (**B**) High-density group in stage 1 above $ECO_{1.4}$. The age-ECD curve of this group (*red curve*) was close to that of stage 0 (*red dotted curve*), and the calculated decrease rate was 0.56%. (**C**) Low-density group in stage 1 below $ECO_{1.4}$. The age-ECD curve of this group (*red curve*) coincided with $ECO_{2.0}$ (*black dotted curve*), with a decrease rate of 2.00%.

spective, hospital-based review of total 1971 outpatients. In this study, we found a somewhat higher prevalence of guttata cornea than that found in previous reports in Japan. The prevalence of corneal guttae was reported to be 3.7% (1.5% in men, 5.5% in women) in Japan,[17,18] whereas it ranges from approximately 7% up to a remarkable 70.4% in North America, Iceland, and Europe.[1,8,19] In our study, the fact that subjects were hospital-based may have caused a higher prevalence. However, such bias does not have an effect on the validity of the mathematical model derived from the data. The following tendency of prevalence was apparent in our group of subjects: First, females were more predisposed to stages 1, 2, and 3 than were males, and the female ratio increased as stages progressed. Second, the prevalence of FCD was much smaller than stage 1. An increase in the female ratio in progressing stages suggested that sex may have some role not only in the onset but also the progression of the disease. Apparent difference of prevalence between FCD and stage 1 suggest the existence of a patient group in stage 1 that does not progress to corneal edema despite having guttata cornea.

Our model is based on the assumptions that the ECD at 5 years of age is common to all classes and that the decrease rate

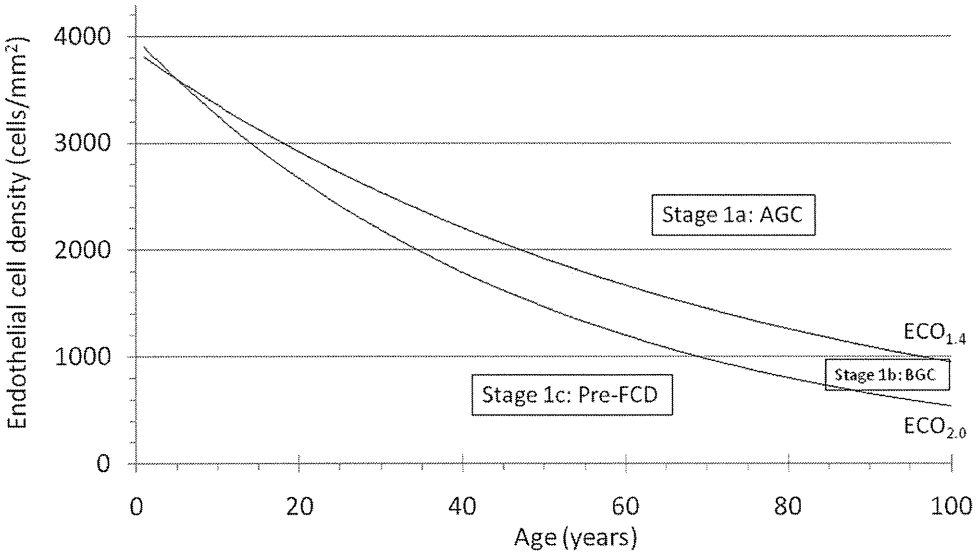

Age (years)		20	30	40	50	60	70	80	90
ECD (cells/mm²)	$ECO_{1.4}$	2918	2537	2205	1917	1667	1449	1260	1095
	$ECO_{2.0}$	2667	2184	1788	1464	1198	981	803	658

FIGURE 3. Proposed classification of eyes in stage 1 based on $ECO_{1.4}$ and $ECO_{2.0}$. Eyes in stage 1a above $ECO_{1.4}$ were named AGC, which had a decrease rate as low as stage 0. Eyes in stage 1c below $ECO_{2.0}$ had a decrease rate as high as FCD (stages 2 and 3), and therefore, this stage was named pre-FCD. Stage 1b between $ECO_{1.4}$ and $ECO_{2.0}$ was named BGC. The table below the graph shows the coordinates of $ECO_{1.4}$ and $ECO_{2.0}$.

of ECD percentage per year) is constant but with a different value of each class. The use of these assumptions may be a debatable point when discussing the validity of our study. However, the results of our mathematical model show ECD decrease rates that are acceptable when compared with clinical observations. The decrease rate of 0.44% in stage 0 is within the range of values of normal unoperated eyes reported in the previous studies.[10,12–16] Furthermore, since $ECO_{1.4}$ and $ECO_{2.0}$ runs through a clearly defined trough between peaks on the scatterplot, and $ECO_{2.0}$ divided stages 0+1 and stages 2+3 or stage 1 and stages 2+3 with high sensitivity and specificity, we believe our mathematical model for classifying patients with guttae based on ECD decrease rates is adequate for predicting the prognosis.

The $ECO_{1.4}$ and $ECO_{2.0}$ curves based on our mathematical model divided stage 1 into three subgroups, stage 1a, 1b, and 1c. The ECD decrease rate of stage 1a was close to that of stage 0, that is, almost normal. Schnitzer and Krachmer reported on 44 relatives of 12 families with guttata cornea which appeared normal on slit-lamp examination and endothelial cell parameters.[20] These eyes presumably belonged to stage 1a of our classification. In addition, because the distribution of patients of stage 1a was located above $ECO_{1.4}$, the risk of progressing to corneal edema may be as low as stage 0. If a patient was on the curve of a 1.4% decrease rate, the ECD would be 1095 cells/mm^2 even when he was 90 years old. Presumption of low risk of stage 1 is supported by analysis of variance, showing that age-ECD curves of each stage had significant predictability.

It was surprising that the age-ECD curve of the low-density group of stage 1 (stages 1b and 1c) coincided completely with $ECO_{2.0}$. The former was calculated by the least-squares method of the low-density group of stage 1, whereas the latter was obtained from trough between peaks of stages 0 to 3 on scatterplots. This result suggests that the low-density group of stage 1 was located on the border between stage 0 and FCD. Eyes in stage 1c below $ECO_{2.0}$ have a decrease rate as high as FCD, suggesting that these eyes have a risk to progress to FCD, even if there was no corneal edema present. This was the rationale for referring to stage 1c as pre-FCD. Further prospective study of patients in stage 1b and 1c is needed to determine whether stage 1c is a preliminary stage of FCD.

Recently, several pathogenic mechanisms, such as oxidative stress or unfolded protein response, have been reported as causes of FCD.[21,22] The difference in resistance against such stress may cause the difference in decrease rates between stages. Previous reports suggested that ECD of some eyes with guttata cornea did not decrease significantly compared with normal eyes after cataract surgery,[7,23] whereas some eyes in other reports showed a significantly higher decrease.[24] When we adapted data from these reports to our classification, we found that most of the former eyes with no difference in ECD (18/21 eyes) were categorized as stage 1a, suggesting that our classification may be used to identify patients with a higher risk of endothelial damage due to external stress. Future studies on guttata corneas using our classification may help clarify the mechanism of FCD progression.

In conclusion, we assessed distribution and endothelial loss rate of guttata cornea stages 0 to 3 and determined new cutoff curves $ECO_{1.4}$ and $ECO_{2.0}$ by using scatterplots. Our mathematical model is a simple method for predicting the prognosis of patients with guttata cornea.

References

1. Weisenthal RW, Streeten BW, eds. *Posterior Membrane Dystrophies.* London: Elsevier Mosby; 2005.
2. Edelhauser HF, Ubels JL, eds. *The Cornea and the Sclera.* 10th ed. ed. St. Louis: Mosby; 2003.
3. Al-Yousuf N, Mavrikakis I, Mavrikakis E, Daya SM. Penetrating keratoplasty: indications over a 10 year period. *Br J Ophthalmol.* 2004;88(8):998–1001.
4. Dobbins KR, Price FW Jr, Whitson WE. Trends in the indications for penetrating keratoplasty in the midwestern United States. *Cornea.* 2000;19(6):813–816.
5. Kang PC, Klintworth GK, Kim T, et al. Trends in the indications for penetrating keratoplasty. 1980–2001. *Cornea.* 2005;24(7):801–803.
6. Krachmer JH, Purcell JJ Jr, Young CW, Bucher KD. Corneal endothelial dystrophy: a study of 64 families. *Arch Ophthalmol.* 1978; 96(11):2036–2039.
7. Kitagawa K, Fujisawa A, Mizuno T, Sasaki K. Twenty-three cases of primary cornea guttata. *Jpn J Ophthalmol.* 2001;45(1):93–98.
8. Adamis AP, Filatov V, Tripathi BJ, Tripathi RC. Fuchs' endothelial dystrophy of the cornea. *Surv Ophthalmol.* 1993;38(2):149–168.
9. Stocker FW. The endothelium of the cornea and its clinical implications. *Trans Am Ophthalmol Soc.* 1953;51:669–786.
10. Murphy C, Alvarado J, Juster R, Maglio M. Prenatal and postnatal cellularity of the human corneal endothelium: a quantitative histologic study. *Invest Ophthalmol Vis Sci.* 1984;25(3):312–322.
11. Nucci P, Brancato R, Mets MB, Shevell SK. Normal endothelial cell density range in childhood. *Arch Ophthalmol.* 1990;108(2):247–248.
12. Cheng H, Jacobs PM, McPherson K, Noble MJ. Precision of cell density estimates and endothelial cell loss with age. *Arch Ophthalmol.* 1985;103(10):1478–1481.
13. Ambrose VM, Walters RF, Batterbury M, Spalton DJ, McGill JI. Long-term endothelial cell loss and breakdown of the blood-aqueous barrier in cataract surgery. *J Cataract Refract Surg.* 1991; 17(5):622–627.
14. Numa A, Nakamura J, Takashima M, Kani K. Long-term corneal endothelial changes after intraocular lens implantation: anterior vs posterior chamber lenses. *Jpn J Ophthalmol.* 1993;37(1):78–87.
15. Bourne WM, Nelson LR, Hodge DO. Central corneal endothelial cell changes over a ten-year period. *Invest Ophthalmol Vis Sci.* 1997;38(3):779–782.
16. Rao SK, Ranjan Sen P, Fogla R, Gangadharan S, Padmanabhan P, Badrinath SS. Corneal endothelial cell density and morphology in normal Indian eyes. *Cornea.* 2000;19(6):820–823.
17. Kitagawa K, Kojima M, Sasaki H, et al. Prevalence of primary cornea guttata and morphology of corneal endothelium in aging Japanese and Singaporean subjects. *Ophthalmic Res.* 2002;34(3): 135–138.
18. Nagaki Y, Hayasaka S, Kitagawa K, Yamamoto S. Primary cornea guttata in Japanese patients with cataract: specular microscopic observations. *Jpn J Ophthalmol.* 1996;40(4):520–525.
19. Zoega GM, Fujisawa A, Sasaki H, et al. Prevalence and risk factors for cornea guttata in the Reykjavik Eye Study. *Ophthalmology.* 2006 Apr;113(4):565–569.
20. Schnitzer JI, Krachmer JH. A specular microscopic study of families with endothelial dystrophy. *Br J Ophthalmol.* 1981;65(6): 396–400.
21. Buddi R, Lin B, Atilano SR, Zorapapel NC, Kenney MC, Brown DJ. Evidence of oxidative stress in human corneal diseases. *J Histochem Cytochem.* 2002;50(3):341–351.
22. Engler C, Kelliher C, Spitze AR, Speck CL, Eberhart CG, Jun AS. Unfolded protein response in Fuchs endothelial corneal dystrophy: a unifying pathogenic pathway? *Am J Ophthalmol.* 2010;149(2):194–202-e2.
23. Stur M, Grabner G, Dorda W. Changes of the corneal endothelium following intracapsular cataract extraction with implantation of semiflexible anterior chamber lenses. I. Results of the early postoperative period. *Acta Ophthalmol (Copenh).* 1984;62(4):586–594.
24. Bourne WM, Nelson LR, Hodge DO. Continued endothelial cell loss ten years after lens implantation. *Ophthalmology.* 1994; 101(6):1014–1022.

Hormonal Regulation of Na^+/K^+-Dependent ATPase Activity and Pump Function in Corneal Endothelial Cells

Shin Hatou, MD†*

Abstract: Na^+- and K^+-dependent ATPase (Na,K-ATPase) in the basolateral membrane of corneal endothelial cells plays an important role in the pump function of the corneal endothelium. We investigated the role of dexamethasone in the regulation of Na,K-ATPase activity and pump function in these cells. Mouse corneal endothelial cells were exposed to dexamethasone or insulin. ATPase activity was evaluated by spectrophotometric measurement, and pump function was measured using an Ussing chamber. Western blotting and immunocytochemistry were performed to measure the expression of the Na,K-ATPase α1-subunit. Dexamethasone increased Na,K-ATPase activity and the pump function of endothelial cells. Western blot analysis indicated that dexamethasone increased the expression of the Na,K-ATPase α_1-subunit but decreased the ratio of active to inactive Na,K-ATPase α_1-subunit. Insulin increased Na,K-ATPase activity and pump function of cultured corneal endothelial cells. These effects were transient and blocked by protein kinase C inhibitors and inhibitors of protein phosphatases 1 (PP1) and 2A (PP2A). Western blot analysis indicated that insulin decreased the amount of inactive Na,K-ATPase α_1-subunit, but the expression of total Na,K-ATPase α_1-subunit was unchanged. Immunocytochemistry showed that insulin increased cell surface expression of the Na,K-ATPase α_1-subunit. Our results suggest that dexamethasone and insulin stimulate Na,K-ATPase activity in mouse corneal endothelial cells. The effect of dexamethasone activation in these cells was mediated by Na,K-ATPase synthesis and an increased enzymatic activity because of dephosphorylation of Na,K-ATPase α_1-subunits. The effect of insulin is mediated by the protein kinase C, PP1, and/or PP2A pathways.

Key Words: corneal endothelium, insulin, ouabain, protein kinase C, protein phosphatase, Na^+- and K^+-dependent ATPase

(*Cornea* 2011;30(Suppl. 1):S60–S66)

A single layer of endothelial cells in a well-arranged mosaic pattern covers the posterior surface of the Descemet membrane in the cornea.[1] Corneal hydration is primarily determined by the balance between penetration of the aqueous humor across the corneal endothelium into the stroma and subsequent pumping of the fluid out of the stroma. The accumulation of fluid in the stroma resulting from disturbance of this balance may lead to bullous keratopathy, which is characterized by an edematous cornea with reduced transparency.[2]

Total pumping activity for the removal of fluid from the cornea is determined by the number of endothelial cells and the pump function of each cell. Given that human corneal endothelial cells have a limited proliferative capacity, endothelial dystrophies, ocular trauma, corneal graft rejection, and insults associated with intraocular surgeries may result in corneal endothelial cell loss and permanent damage. Replacement of the corneal endothelium by keratoplasty is currently the only established therapeutic approach for recovery of endothelial cell number. Pseudophakic or aphakic bullous keratopathy, Fuchs endothelial dystrophy, and failed corneal grafts remain common indications for keratoplasty, accounting for approximately 60% of the total number of such procedures.[3–5] Activation of the pump function in the remaining endothelial cells is a potential alternative approach to recovery of the total pumping activity in the cornea, so long as the total number of such cells is within an acceptable range. However, therapeutic approaches to the activation of corneal endothelial cells remain to be established.

The Na^+- and K^+-dependent ATPase (Na,K-ATPase) expressed in the basolateral membrane of corneal endothelial cells is primarily responsible for the pump function of the corneal endothelium.[1] The Na,K-ATPase pump site density in the corneal endothelium was found to be increased in eyes affected by moderate guttata.[6] Na,K-ATPase pump site density showed an initial increase, a sudden marked decrease, and a subsequent gradual decline associated with the end stage of disease in patients with Fuchs endothelial dystrophy.[7] These observations indicate that certain conditions can induce a compensatory increase in Na,K-ATPase pump site density and, presumably, in endothelial pump function. They also suggest the existence of a regulatory mechanism, or mechanisms, for the control of total Na,K-ATPase activity in the corneal endothelium.

Several studies have shown that glucocorticoids stimulate Na,K-ATPase activity through multiple complex mechanisms, including gene expression, transcription, translocation, and enzymatic activity, in a variety of tissues.[8] Although the results of experimental studies concerning the effects of glucocorticoids on corneal endothelial damage do not show any close correlations,[9–11] topical glucocorticoids have been clinically used for the treatment of corneal

From the *Division for Vision Research, National Institute of Sensory Organs, National Tokyo Medical Center, Tokyo, Japan; and †Department of Ophthalmology, Keio University School of Medicine, Tokyo, Japan.
Supported in part by a grant from the Ministry of Health, Labour and Welfare (Japan).
The author has no financial or conflicts of interest to disclose.
Reprints: Shin Hatou, Department of Ophthalmology, Keio University School of Medicine, 35 Shinanomachi, Shinjuku-ku, Tokyo 160-8582, Japan (e-mail: tr97469@zc4.so-net.ne.jp).

endothelial disorders. Indeed, steroid administration seemed to increase endothelial pump function and ameliorate stromal edema in a patient with bullous keratopathy secondary to Sato refractive surgery.[12] In contrast, clinical observations of a higher incidence of persistent corneal edema after vitrectomy and other surgical procedures for patients with diabetes mellitus have suggested that abnormal corneal endothelial function is associated with diabetes mellitus.[13–18] Specular microscopic studies have shown morphological abnormalities, such as lower endothelial cell density and increased endothelial pleomorphism, in patients with types 1 and 2 diabetes mellitus.[18–27] Some clinical studies have shown that diabetic patients tend to have slightly thicker corneas and a reduced recovery rate from hypoxia-induced corneal edema.[28–31] These observations led us to the idea that Na,K-ATPase activity and pump function of the corneal endothelium may be affected by several hormones, such as glucocorticoids or insulin.

In this review, we outline methods for measuring the enzymatic activity and pump function of Na,K-ATPase in cultured mouse corneal endothelial cells. This is followed by a review of the roles of dexamethasone and insulin in controlling the enzymatic activity and pump function of Na,K-ATPase in corneal endothelial cells. Additionally, we present the mechanisms by which dexamethasone or insulin might affect Na,K-ATPase activity.

MEASUREMENT OF Na,K-ATPase ENZYME ACTIVITY

Corneal endothelial cells were cultured with or without dexamethasone, insulin, staurosporine, GF109203X, or okadaic acid. To measure Na,K-ATPase enzyme activity, ouabain (final concentration, 1 mM) or vehicle was added to cell cultures and incubated for 30 minutes at 37°C. After further addition of adenosine triphosphate (final concentration, 10 mM), the adenosine triphosphate hydrolysis reaction catalyzed by Na,K-ATPase released phosphate. The concentration of phosphate was determined by spectrophotometric measurement with ammonium molybdate. The Na,K-ATPase activity was calculated as the difference in phosphate concentration between cells with and without ouabain.

MEASUREMENT OF ELECTRICAL Na,K-ATPase PUMP FUNCTION

To measure pump function, cells cultured on Snapwell inserts were placed in an Ussing chamber. The endothelial cell surface side was in contact with 1 chamber and the Snapwell membrane side was in contact with another chamber. If Na,K-ATPase was active, then a short-circuit current would be evoked by active sodium and potassium flux. After the short-circuit current had reached a steady state, ouabain was added. The pump function attributable to Na,K-ATPase activity was calculated as the difference in short-circuit current measured before and after the addition of ouabain (Fig. 1).

DEXAMETHASONE STIMULATES Na,K-ATPase ACTIVITY

Mouse corneal endothelial cells were exposed to 10 μM dexamethasone for various periods and Na,K-ATPase activity was then measured. Dexamethasone increased Na,K-ATPase activity in a time-dependent manner, with this effect being significant ($P < 0.05$; Student t test) at 6 hours and maximal at 48 hours (Fig. 2). The stimulatory effect of dexamethasone on Na,K-ATPase activity was also concentration dependent (Fig. 2).[32] The stimulatory effect of dexamethasone on pump function was time dependent, being significant at 24 hours and maximal at 48 hours (Fig. 3A),[32] and concentration dependent, which was apparent at 1 or 10 μM (Fig. 3B).[32] These results were similar to those obtained for Na,K-ATPase activity.

To determine whether dexamethasone affects Na,K-ATPase expression in corneal endothelial cells, we exposed the cells to dexamethasone for 48 hours and measured the expression of total Na,K-ATPase α_1-subunit and phospho-Na,K-ATPase α_1-subunit by Western blot analysis. Phospho-Na,K-ATPase α_1-subunit is considered to be the inactive state of the Na,K-ATPase α_1-subunit. Levels of the Na,K-ATPase α_1-subunit and phospho-Na,K-ATPase α_1-subunit were measured and are presented as relative amounts compared with the signal intensities for β-actin (Fig. 4A).[32] Dexamethasone increased the expression of total Na,K-ATPase α_1-subunit in a concentration-dependent manner, whereas it did not alter the expression of the phospho-Na,K-ATPase α_1-subunit (Figs. 4B, C)[32]; therefore, the ratio of phospho-Na,K-ATPase α_1-subunit expression to total Na,K-ATPase α_1-subunit expression was decreased in a concentration-dependent manner (Fig. 4D).[32]

INSULIN TRANSIENTLY ACTIVATES Na,K-ATPase

To determine whether insulin affects Na,K-ATPase activity in corneal endothelial cells, we exposed the cells to 0.1 μM insulin for various periods and measured the

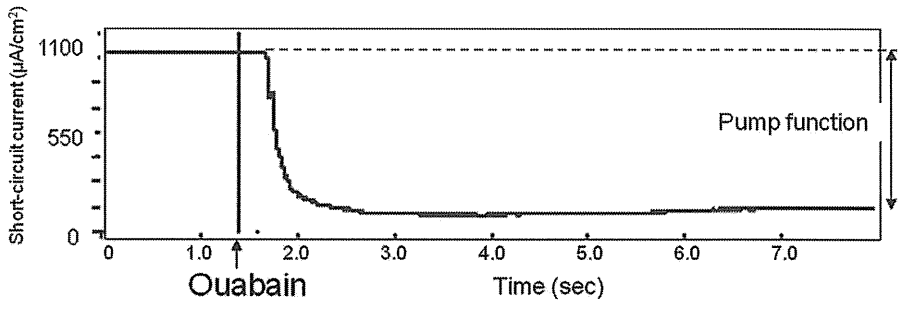

FIGURE 1. Representative trace of short-circuit current (microamperes per well) obtained with cell monolayers in an Ussing chamber. The insert well membrane growth area was 4.67 cm^2. Pump function attributable to Na,K-ATPase activity was calculated as the difference in short-circuit currents obtained before and after the addition of ouabain.

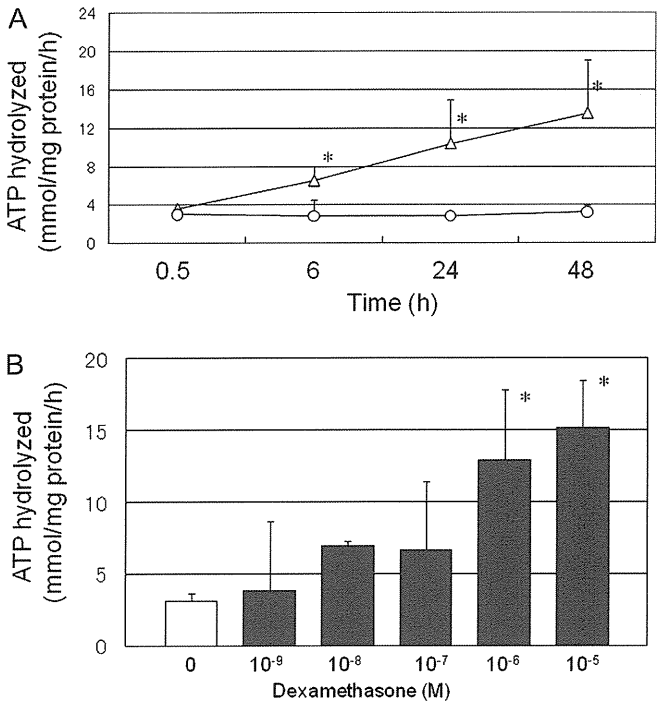

FIGURE 2. Effect of dexamethasone on Na,K-ATPase activity in cultured mouse corneal endothelial cells. A, Cells were incubated in the absence (circles) or presence (triangles) of 10 μM dexamethasone for the indicated times and then assayed for Na,K-ATPase activity. *$P < 0.05$ versus the corresponding value for cells incubated without dexamethasone (Student t test). B, Cells were incubated with the indicated concentrations of dexamethasone for 48 hours and then assayed for Na,K-ATPase activity. *$P < 0.01$ for the indicated comparisons (Student t test). Modified with permission from Hatou et al.[32]

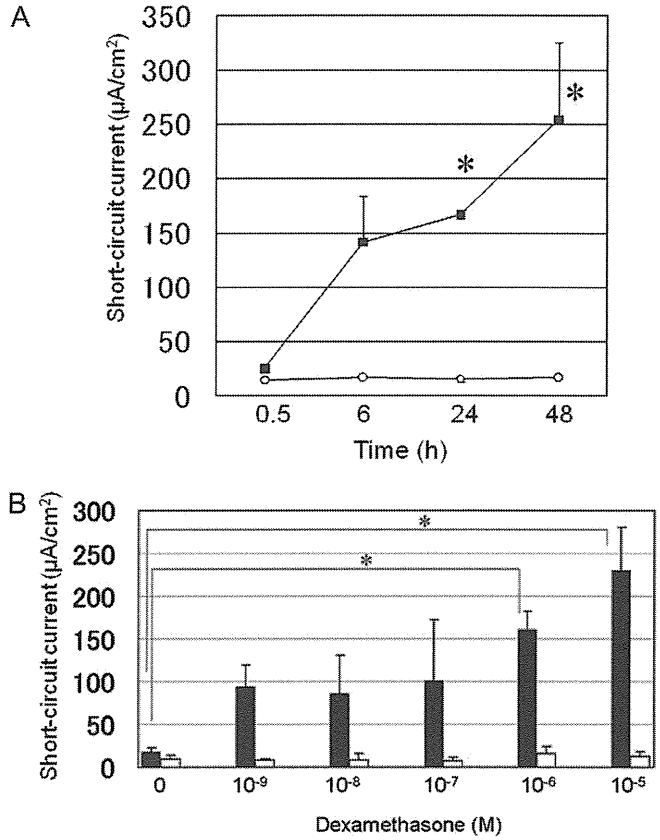

FIGURE 3. Effect of dexamethasone on the pump function of cultured mouse corneal endothelial cells. A, Cells were incubated in the absence (circles) or presence (squares) of 10 μM dexamethasone for the indicated times and then assayed for pump function (microamperes per square centimeter). *$P < 0.05$ versus the corresponding value for cells incubated without dexamethasone (Student t test). (B) Pump function (microamperes per square centimeter) attributable to Na,K-ATPase activity was determined 48 hours after incubation of cells in the presence of the indicated concentrations of dexamethasone (black). Ouabain-independent short-circuit current (white) is also presented, which did not change significantly with the indicated concentrations of dexamethasone. Data are means ± SDs of values from 4 replicate experiments. *$P < 0.05$ for the indicated comparisons (Student t test). Modified with permission from Hatou et al.[32]

Na,K-ATPase activity. Insulin had a transient stimulatory effect on Na,K-ATPase activity, with this effect being significant at 6 and 12 hours. After 12 hours, Na,K-ATPase activity returned to baseline levels. The stimulatory effect of insulin on Na,K-ATPase activity was also concentration dependent (Fig. 5).[33]

We next examined whether insulin affects the pump function of corneal endothelial cells. Insulin at 0.1 μM increased the ouabain-sensitive pump function of the corneal endothelial cells compared with control cells. This effect of insulin was statistically significant ($P < 0.05$) at 6 hours. The stimulatory effect of insulin on pump function was concentration dependent, and these results were similar to the results obtained for Na,K-ATPase activity (Fig. 6).[33]

PROTEIN KINASE C MEDIATION OF INSULIN-INDUCED Na,K-ATPase ACTIVATION

To test whether the stimulatory effect of insulin on Na,K-ATPase activity was mediated by protein kinase C (PKC), we examined the effects of staurosporine and GF109203X. The increase in Na,K-ATPase activity induced by insulin was significantly inhibited ($P < 0.01$) by staurosporine and GF109203X (Fig. 7).[33] We next examined whether okadaic acid affected the Na,K-ATPase activation induced by insulin. The activity of Na,K-ATPase in conjunction with 0.1 μM insulin was significantly reduced ($P < 0.01$) in the presence of 1 μM okadaic acid (Fig. 7).[33]

We exposed cells to 0.1 μM insulin for 6 hours and then measured the expression levels of total Na,K-ATPase α_1-subunit and phospho-Na,K-ATPase α_1-subunit by Western blotting to determine whether insulin affected Na,K-ATPase expression in corneal endothelial cells. Although there was no statistically significant difference in the expression of total Na,K-ATPase α_1-subunit (Fig. 8A, B),[33] insulin significantly decreased ($P < 0.05$) the ratio of phospho-Na,K-ATPase α_1-subunit expression to total Na,K-ATPase α_1-subunit (Fig. 8C).[33]